that these cell lines expressed higher levels of the liver-specific genes than the HEK293 cells used as negative controls (Fig. 1A). These results suggested that the expression of AFP was correlated with that of the examined liver-specific host factors in cancer cell lines. Next, to confirm this correlation, the expression levels of ALB, ApoB, ApoE, MTTP, and miR-122 were determined by qPCR in AFP-expressing cell lines, including FU97, OV-90, and HCC-derived Huh7, HepG2, Hep3B, and JHH-4 cells (Fig. 1B). Takigawa cells were difficult to culture, and Caco-2 cells have previously been reported to permit entry and replication of HCV (42, 43); therefore, we excluded these cell lines for further analyses. JHH-4 cells were previously shown to permit a partial propagation of HCV in a three-dimensional cultivation by using a radial-flow bioreactor system upon inoculation with plasma from an HCV carrier (44). In contrast to 293T cells, these AFP-expressing cell lines express high levels of the examined liver-specific host factors, suggesting that these cell lines maintain their hepatic functions. Because previous studies have shown that Huh7, HepG2, and Hep3B cells are susceptible to HCVcc infection, we selected JHH-4, FU97, and OV-90 cells for further investigation as new cell line candidates for HCV propagation. It is well known that hepatocytes and intestinal cells produce ApoB100 and ApoB48, respectively. ApoB100 was detected in the culture supernatants of Huh7, JHH-4, FU97, and OV-90 cells but not in those of 293T cells by immunoblotting (Fig. 1C). These results suggest that FU97 and OV-90 cells are differentiated into hepatocyte-like cells and possess liver-specific functions. The expression of entry receptor molecules for HCV, including hCD81, CLDN1, OCLN, and SR-BI (45–48), in these cell lines was confirmed by immunoblotting and fluorescence-activated cell sorting (FACS) analyses (Fig. 1D and E). To further determine the authenticity of the receptor candidates for HCV entry, HCVpv was inoculated into these cell lines. Although the infectivity of HCVpv to JHH-4 and FU97 cells was comparable to that in Huh7 cells, OV-90 cells did not show any susceptibility to HCVpv infection (Fig. 1F). Cell surface expression of CLDN1 and OCLN was detected in OV-90 cells (data not shown); therefore, lack of susceptibility of OV-90 cells to HCVpv infection might be attributable to lower expression of SR-B1 and hCD81 in OV-90 cells than in other cell lines (Fig. 1D and E). Thus, we selected JHH-4 and FU97 cells for further investigation of HCV propagation.

JHH-4 and FU97 cells permit HCV propagation. To examine the susceptibility of JHH-4 and FU97 cells to HCV propagation, HCVcc was inoculated into these cells at a multiplicity of infection (MOI) of 1, and intracellular HCV RNA and infectious titers in the culture supernatants were determined by qRT-PCR and focus-forming assay, respectively. FU97 cells exhibited higher levels of HCV gene expression than JHH-4 cells, and these levels increased continuously until 48 h postinfection; treatment with IFN-α significantly inhibited HCV gene expression in both JHH-4 and FU97 cells (Fig. 2A, left panels). In addition, substantial amounts of infectious particles were detected in the culture supernatants of JHH-4 and FU97 cells infected with HCVcc, in contrast to the lack of infectious particles in the culture supernatants of 293T-CLDN/miR-122 cells infected with HCVcc (Fig. 2A, bar graph). Recent reports have shown that exogenous expression of miR-122 enhances HCV RNA abundances in several hepatic or nonhepatic cell lines (16–18). Therefore, we examined the effect of miR-122 overexpression on HCV RNA abundances in both JHH-4 and FU97 cells. miR-122 was introduced in these cells by a lentiviral vector encoding pri-miR-122, an unprocessed miR-122, and miR-122 expression was confirmed by quantitative PCR (qPCR) analysis (Fig. 2B, bar graph). In contrast to the slight increase of HCV RNA in FU97 cells, JHH-4 cells exhibited a significant increase of HCV RNA, suggesting that the expression level of miR-122 is a key determinant for the efficient propagation of HCV (Fig. 2B, right panels). A previous study has shown that NS5A proteins were localized around the endoplasmic reticulum (ER) membrane, and accumulation of core protein around lipid droplets (LDs) facilitates efficient assembly of infectious particles in Huh7 cells (24). Immunofluorescence microscopy observation revealed that core and NS5A proteins in JHH-4 and FU97 cells infected with HCVcc were detected around LDs and in the ER together with double-stranded RNA (dsRNA), respectively (Fig. 2C). These results suggest that expression of liver-specific factors permits complete propagation of HCVcc in JHH-4 and FU97 cells and that hepatic characteristics play crucial roles in HCV propagation.

JHH-4 and FU97 cells permit complete propagation of HCVcc without any exogenous expression of host factors crucial for propagation of HCV. To further characterize the propagation of HCV in JHH-4 and FU97 cells, we examined the effects of the HCV inhibitors on the replication of HCV RNA. Preincubation with anti-HCV E2 antibody and pretreatment of cells with anti-hCD81 monoclonal antibody significantly inhibited HCVcc infection not only in Huh7 cells but also in JHH-4 and FU97 cells, suggesting that hCD81 is also involved in HCV entry into JHH-4 and FU97 cells (Fig. 3A, left panels). To examine the effect of miR-122 expression on HCV RNA abundances, cells were treated with LNA specific to either miR-122 (miR-122–LNA) or a non-specific LNA (Ctrl-LNA) at 6 h before infection with HCVcc. Treatment with miR-122–LNA but not with Ctrl-LNA significantly reduced the HCV RNA abundances in these cell lines, suggesting that miR-122 also plays a crucial role in the efficient propagation of HCVcc in JHH-4 and FU97 cells (Fig. 3A, right panels). Previous reports showed that treatment with MTTP inhibitors inhibited the production of infectious particles of HCVcc in Huh7 cells (20, 22). Although intracellular HCV RNA levels in Huh7, JHH-4, and FU97 cells were not inhibited by the treatment with MTTP inhibitors, including CP-346086 and BMS-200150 (Fig. 3B, left panels), the production of infectious particles was significantly decreased in these cells (Fig. 3B, right panels). These results suggest that the VLDL secretion pathway also participates in the propagation of HCV in JHH-4 and FU97 cells. Furthermore, it was shown that ApoB and ApoE are involved in the production of HCV particles in Huh7 cells (20–22). To confirm the role of ApoB and ApoE in HCV propagation in JHH-4 and FU97 cells, the expression of ApoB and ApoE was suppressed by siRNAs (Fig. 3C, left panels). The suppression of ApoB and ApoE expression significantly reduced HCV RNA levels in cells infected with HCVcc at an MOI of 1 (Fig. 3C, middle panels) and significantly reduced the infectious titers in the supernatants (Fig. 3C, right panels) at 72 h postinfection. Collectively, these results suggest that the JHH-4 and FU97 cells permit complete propagation of HCVcc without any exogenous expression of the host factors crucial for propagation of HCV, including receptor molecules, miR-122, and VLDL-associated proteins. FU97 cells exhibited higher susceptibility to HCVcc propagation than JHH-4 cells (Fig. 2A), and thus we characterized the FU97 cells in greater detail.

Establishment of HCV RNA replicon and cured cells by using FU97 cells. To further examine the characteristics of FU97 cells

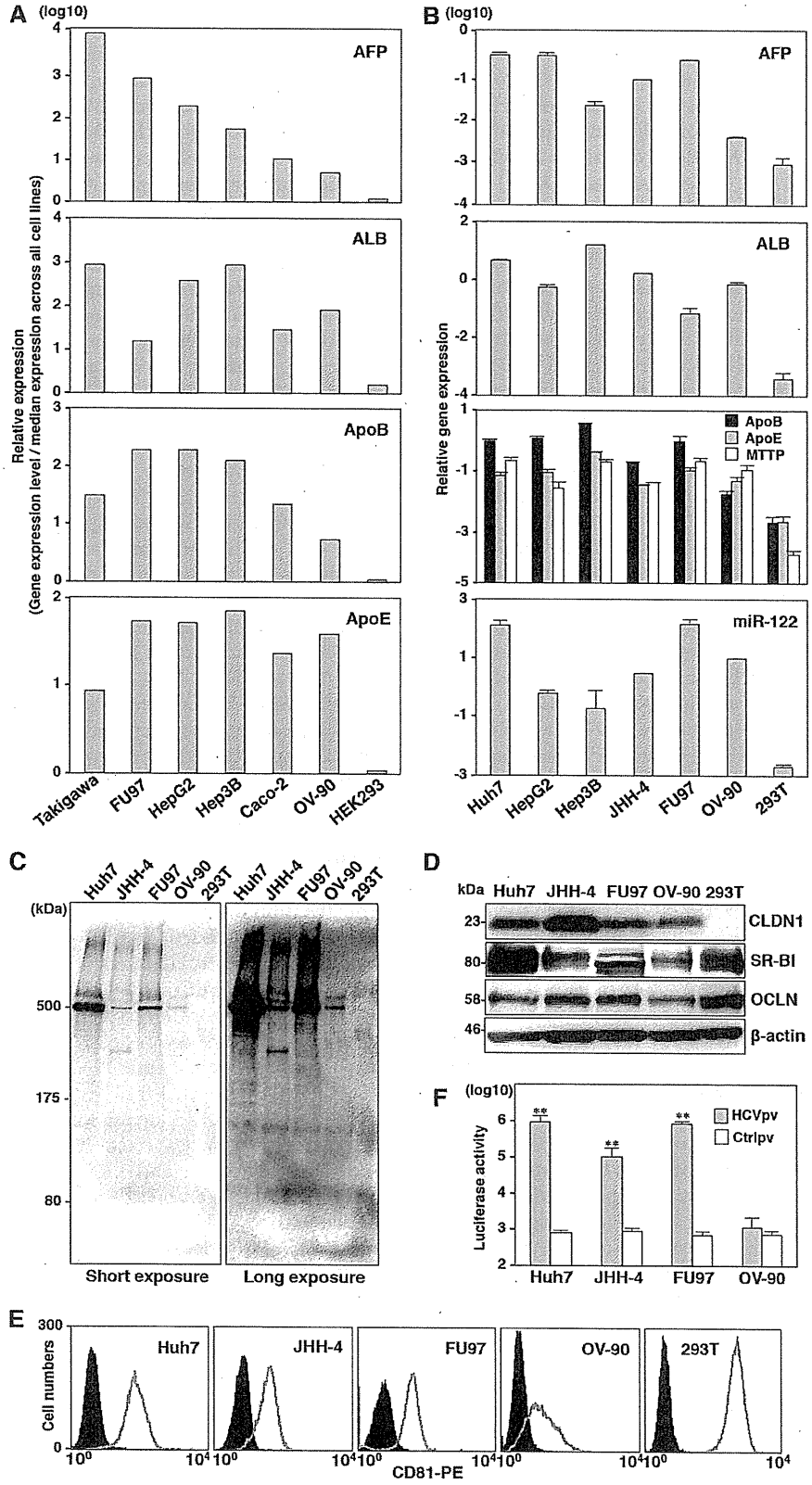

FIG 1 JHH-4 and FU97 cells express high levels of the liver-specific host factors required for HCV propagation. (A) Expression of AFP, ALB, ApoB, and ApoE in cancer cell lines screened by the NextBio Body Atlas application. The expression levels were standardized by the median expression across all cell lines. (B) Expression of AFP, ALB, ApoB, ApoE, MTTP, and miR-122 in AFP-expressing cell lines including HepG2, Hep3B, FU97, and OV-90 cells identified by NextBio

with respect to HCV RNA replication, *in vitro*-transcribed subgenomic HCV RNA of the Con1 strain was electroporated into Huh7 and FU97 cells and cultured in medium containing G418 for a month, and then subgenomic replicon (SGR) cells of the Con1 strain were established (Fig. 4A). Replication of HCV RNA in four clones of the FU97 replicon cells was examined by qRT-PCR and immunoblotting. All clones contained a high level of HCV RNA (3×10^7 to 7×10^7 copies/μg total RNA) (Fig. 4B, upper panel), and the NS5A protein was also detected (Fig. 4B, lower panel). We examined the localization of NS5A and dsRNA in clone 5 of FU97 SGR cells by immunofluorescence analysis. Colocalization of NS5A with dsRNA was observed in clone 5, suggesting that the replication complex required for viral RNA replication was generated in the FU97 SGR cells (Fig. 4C). It has been shown that the infectivity of HCVcc in the cured cells that were established by elimination of the viral genome by treatment with antivirals from Huh7 replicon cells is significantly higher than that in parental Huh7 cells (49). To establish FU97 cured cells, two clones of FU97 replicon cells (clones 5 and 7) were treated with a combination of either 100 IU/ml of IFN-α and 100 nM BILN 2061 (clones 5-1 and 7-1) or 10 pM BMS-790052 and 100 nM BILN 2061 (clones 5-2 and 7-2) to eliminate viral RNA. Viral RNA was gradually decreased and was completely eliminated at 26 days posttreatment in four clones (Fig. 4D), and elimination of NS5A expression in cured cells was confirmed by immunoblot analysis (Fig. 4E). Next, to examine the susceptibility of the cured cells to the propagation of HCVcc, FU97 cured cell clones (clones 5-1 and 7-1) and parental FU97 cells were infected with HCVcc at an MOI of 1. The cured cells are more permissive to HCV infection, resulting in increased HCV RNA (Fig. 4F) and NS5A abundances (Fig. 4G) compared to the parental cells. These results suggest that susceptibility of the cured FU97 cells to the propagation of HCVcc is higher than that of parental cells, as seen in previous studies using hepatic and nonhepatic cells (17, 18, 49).

Cured FU97 cells exhibit normal innate immune response. It has been shown that one of the reasons for the high susceptibility of the cured cell line, Huh7.5 cells, to HCVcc infection is the impairment of the innate immune responses caused by mutation in RIG-I, a key sensor for viral RNA (50). To examine the involvement of the innate immune response in the enhancement of HCVcc propagation in the cured FU97 cells, the expression levels of IFN-stimulated gene 15 (ISG15) were determined upon stimulation with IFN-α or infection with VSV. Expression of ISG15 was significantly increased in both parental and cured FU97 cells by treatment with IFN-α or infection with VSV (Fig. 5A). To further confirm the innate immune responses in the cured FU97 cells, reporter plasmids encoding the luciferase gene under the control of either the IFN-β (Fig. 5B, left) or ISRE (Fig. 5B, right) promoter were transfected into both parental and cured FU97 cells and treated with IFN-α or inoculated with VSV. Activation of these promoters in the cured cells was comparable to that in the parental cells. To further assess the authenticity of viral RNA recognition and ISG induction pathways in the cured cells, nuclear localization of IRF3 and STAT2 upon stimulation was determined by immunofluorescence analysis. IRF3 and STAT2 in both parental and cured FU97 cells were translocated at similar levels into the nucleus upon infection with VSV or treatment with IFN-α (Fig. 5C). These results suggest that the efficient propagation of HCVcc in the FU97 cured cells is attributable to reasons other than impairment of innate immunity.

Expression of miR-122 is one of the determinants for HCV RNA abundances. We hypothesized that HCV replicon cells are capable of surviving in the presence of G418 by amplification of the viral genome through the enhancement of miR-122 expression, and cured FU97 cells acquired the ability to propagate HCVcc due to the high-level expression of miR-122. Our previous study also suggested that the expression levels of miR-122 in Huh7, Hep3B, and Hec1B cured cells were higher than those in parental cells (17, 18). To test this hypothesis, the expression levels of miR-122 in the cured FU97 cells were compared with those in parental cells. Interestingly, the cured FU97 cell clones exhibited a 1.8-fold increase in miR-122 expression (Fig. 6A). These results suggested that the efficient propagation of HCVcc in the cured FU97 cells was attributable to enhanced expression of miR-122 rather than the impairment of the innate immunity. To further confirm the correlation between the expression of miR-122 and HCV RNA abundances, we established FU97 cell lines expressing various concentrations of miR-122 by using a lentiviral vector (Fig. 6B), and HCV RNA abundances in these cell lines upon infection with HCVcc were determined by qRT-PCR (Fig. 6C). HCV RNA abundances increased in accord with the expression of miR-122, suggesting that expression of miR-122 is one of the determinants for HCV RNA abundances in cells infected with HCVcc.

HCV particles produced in FU97 cells exhibit similar characteristics to those in hepatic cells. To examine the characteristics of viral particles produced in FU97 cells, HCV particles recovered from the culture supernatants of Huh7.5.1 and FU97 cells infected with HCVcc were fractionated by buoyant density gradient analysis. Previous reports indicated that viral RNA and infectious particles were broadly distributed, with peaks in fractions from 1.13 to 1.14 g/ml and from 1.09 to 1.10 g/ml, respectively (51, 52). In agreement with the previous data, major peaks of HCV RNA and infectious particles in culture supernatants of both Huh7.5.1 and FU97 cells were detected around 1.10 g/ml and 1.09 g/ml, respectively (Fig. 7A and 7B, upper panels). Furthermore, ApoE was detected around the peak fractions of infectivity in both Huh7.5.1 and FU97 cells (Fig. 7A and B, lower panels). These results suggest that HCV particles produced in FU97 cells exhibit characteristics similar to those in hepatic cells.

Effects of anti-HCV drugs on the propagation of HCV in FU97 cells. To determine the difference in the efficacies of antivirals on the HCV propagated in Huh7 and FU97 cells, three DAAs, i.e., BMS-790052, PSI-7977, and BILN 2061 targeting NS5A,

Body Atlas and Huh7, JHH-4, and 293T cells was determined by qPCR. The relative expression of AFP, ApoB, ApoE, MTTP, and ALB mRNA was normalized to that of glyceraldehyde-3-phosphate dehydrogenase (GAPDH) mRNA, and that of miR-122 was normalized to that of U6 snRNA. (C) Secretion of ApoB in the culture supernatants of Huh7, JHH-4, FU97, OV-90, and 293T cells was determined by immunoblotting by using anti-ApoB antibody. The molecular mass of ApoB100 secreted from hepatocyte is about 500 kDa. (D) Expression of CLDN1, SR-BI, and OCLN in these cell lines was determined by immunoblotting. (E) Expression of hCD81 in the cell lines was determined by flow cytometry. (F) HCVpv-bearing HCV envelope proteins and control virus (Ctrlpv) were inoculated into the cell lines, and luciferase activities were determined at 24 h postinfection. Asterisks indicate significant differences (*, $P < 0.05$; **, $P < 0.01$) versus the results for control virus.

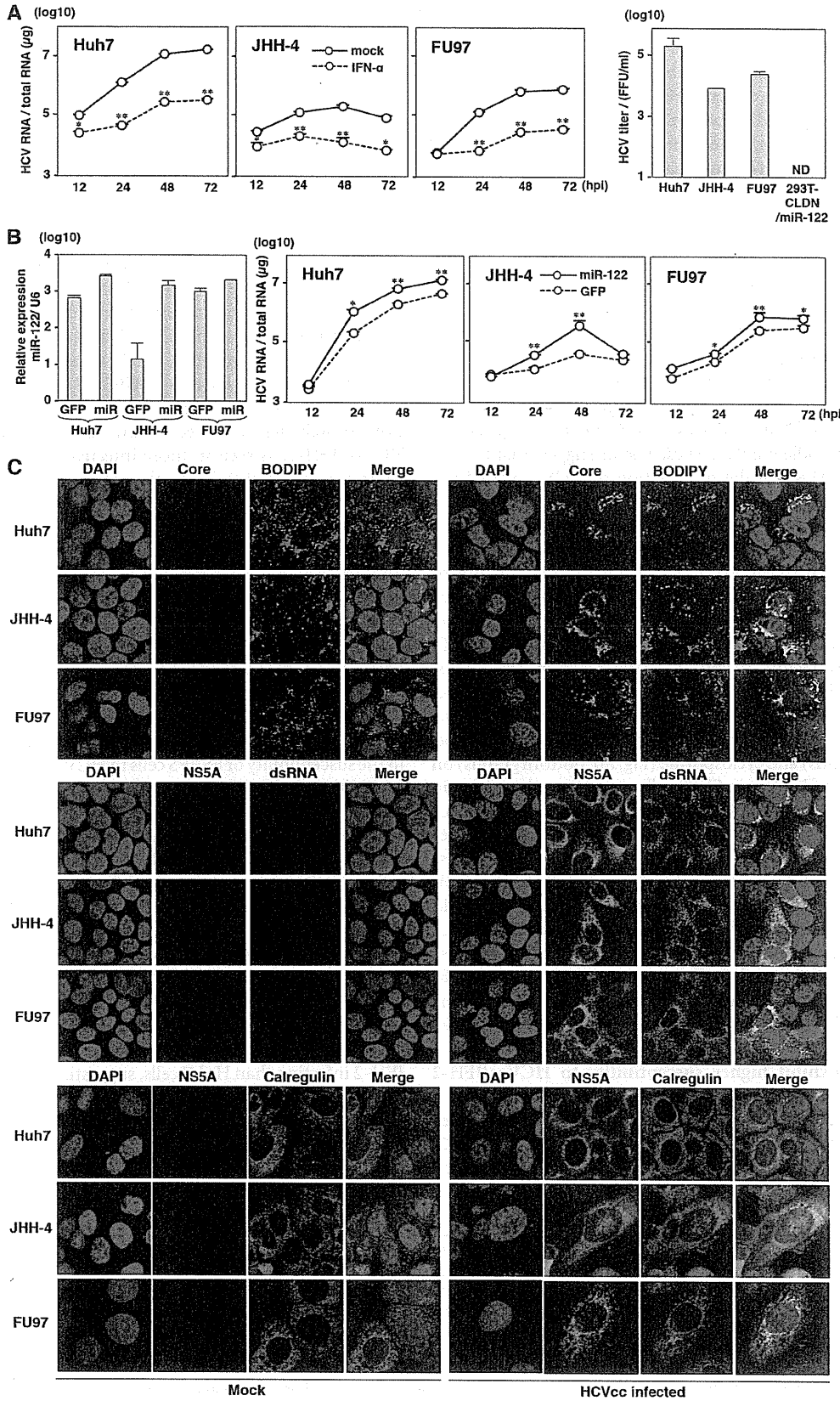

NS5B, and NS3/4A, respectively, were treated with various concentrations at 3 h postinfection with HCVcc, and the intracellular HCV RNA level was determined by qRT-PCR at 48 h postinfection. Treatment with these DAAs inhibited the HCV RNA level in a dose-dependent manner in both Huh7 and FU97 cells (Fig. 8A, bar graphs) and exhibited no cell toxicity at all even at the highest dose (Fig. 8A, line graphs). The inhibitory effects of BMS-790052 (Fig. 8A, top graphs) on the propagation of HCVcc in FU97 cells were higher than those in Huh7 cells, and the 50% effective concentration (EC_{50}) values of BMS-790052 against propagation of HCVcc in FU97 and Huh7 cells were 7.2 and 21.8 pM, respectively ($P < 0.05$). On the other hand, the antiviral effects of BILN 2061 (Fig. 8A, bottom graphs) on the propagation of HCVcc in FU97 cells were lower than those in Huh7 cells, and EC_{50}s of BILN 2061 against propagation of HCVcc in FU97 and Huh7 cells were 65.0 and 38.9 nM, respectively ($P < 0.01$). PSI-7977 showed almost equivalent inhibitory effects to HCV propagated in FU97 and Huh7 cells, and the EC_{50}s of PSI-7977 against propagation of HCVcc in FU97 and Huh7 cells were 34.6 and 44.1 nM, respectively (Fig. 8A, middle graphs). These results suggest that the antiviral effect of DAAs on the propagation of HCVcc varied between Huh7 and FU97 cells.

Next, we examined the efficacy of IFN-α, RBV, and cyclosporine, which are inhibitors for HCV targeting host factors involved in the propagation of HCVcc (53–55), on the propagation of HCVcc in Huh7 and FU97 cells. Cells were treated with various concentrations of the reagents at 3 h postinfection with HCVcc, and the level of intracellular HCV RNA was determined by qRT-PCR at 48 h postinfection. In contrast to the treatment with DAAs, both Huh7 and FU97 cells exhibited cell toxicity by the treatment with RBV and cyclosporine but not with IFN-α at higher concentrations (Fig. 6B, line graphs). The inhibitory efficacies of IFN-α (Fig. 8B, top graphs) and cyclosporine (Fig. 8B, bottom graphs) on the propagation of HCVcc in FU97 cells were lower than those in Huh7 cells, and the EC_{50}s of IFN-α against propagation of HCVcc in FU97 and Huh7 cells were 4.3 and 2.5 IU/ml, ($P < 0.05$), respectively; those of cyclosporine were 6.9 and 3.2 μg/ml ($P < 0.01$), respectively. On the other hand, the antiviral effect of RBV on the propagation of HCVcc in FU97 cells was higher than that in Huh7 cells, and the EC_{50}s of RBV against propagation of HCVcc in FU97 and Huh7 cells were 99.0 and 198.9 μM, respectively ($P < 0.05$) (Fig. 8B, middle graphs). These results suggest that the efficacies of anti-HCV drugs targeting host factors involved in the infection of HCV were also different between Huh7 and FU97 cells.

FU97 cells exhibit higher susceptibility to HCVcc/JFH-2 propagation than Huh7 cells. HCVcc/JFH-2 was cloned from a patient with fulminant hepatitis and exhibited efficient propagation in Huh7 cured cells (34). *In vitro*-transcribed RNA of pJFH2/AS/mtT4 encoding a full-length JFH-2 strain was electroporated into Huh7.5.1 cells, and HCVcc/JFH-2 of 1.5×10^5 FFU/ml was recovered in the supernatants after serial passages. To examine the susceptibility of FU97 cells to the propagation of HCVcc/JFH-2, cells were infected with HCVcc/JFH-2 at an MOI of 1, and the intracellular HCV RNA level was determined by qRT-PCR. Intracellular HCV RNA in parental and cured FU97 cells increased until 72 h postinfection, while it reached a peak at 48 h postinfection in Huh7 cells, and the highest HCV RNA level was observed in the cured FU97 clones upon infection with HCVcc/JFH-2 (Fig. 9A). Infectious titers in the culture supernatants at 72 h postinfection with HCVcc/JFH-2 were also highest in the cured FU97 7-1 cells (2.5×10^4 FFU/ml), followed by parental FU97 (1.2×10^4 FFU/ml) and Huh7 (9×10^3 FFU/ml) cells (Fig. 9B). Next, we examined the expression and subcellular localization of HCV proteins in cells infected with HCVcc/JFH-2 by immunofluorescence analysis. Expression of NS5A in cells upon infection with HCVcc/JFH-2 was highest in the cured FU97 7-1 cells, followed by parental FU97 cells, and that in Huh7 cells was low (Fig. 9C, left panels). Core protein was detected around LDs in cells infected with HCVcc/JFH-2, as seen in those infected with the HCVcc/JFH-1 strain (Fig. 9C, right). To further confirm the efficient propagation of HCVcc/JFH-2 in FU97 cells, *in vitro*-transcribed viral RNAs of the JFH-1 and JFH-2 strains of HCVcc were electroporated into Huh7, FU97, and cured FU97 cells. Although the infectious titers of the JFH-1 strain in FU97 cells were lower than those in Huh7 cells, those of the JFH-2 strain in FU97 and cured FU97 cells were significantly higher than those in Huh7 cells (Fig. 9D). These results suggest that FU97 cells are more susceptible to propagate HCVcc/JFH-2 than Huh7 cells.

DISCUSSION

Several reports have shown that hepatic differentiation is involved in the susceptibility of ES/iPS cells to HCVcc infection (28, 30, 41). In addition, in hepatic cancer cell lines, including Huh7, HepG2, and Hep3B, cells derived from not poorly but well-differentiated HCC permit complete propagation of HCVcc (15–17), suggesting that hepatic differentiation is closely related to the susceptibility of cells to HCVcc propagation. In this study, we identified two cell lines susceptible to HCVcc infection by the screening of cancer cell lines expressing AFP as a marker of hepatic differentiation. HCC-derived JHH-4 cells and gastric cancer-derived FU97 cells permit complete propagation of HCVcc without any exogenous expression of the host factors required for HCVcc propagation, including HCV receptor candidates, miR-122, and apolipoproteins. In particular, FU97 cells exhibited higher susceptibility to HCVcc/JFH-2 infection than Huh7 cells, suggesting that FU97 cells would be useful tools for further HCV analyses.

Although HCV has been classified into seven major genotypes and a series of subtypes (56, 57), the *in vitro* infection model had been restricted to the JFH-1 strain based on the genotype 2a until

FIG 2 JHH-4 and FU97 cells permit HCV propagation. (A) Intracellular HCV RNA levels in Huh7, JHH-4, and FU97 cells inoculated with HCVcc at an MOI of 1, treated with 100 IU/ml of IFN-α or untreated (mock), were determined by qRT-PCR at 12, 24, 48, and 72 h postinfection (hpi). Infectious titers in the culture supernatants of Huh7, JHH-4, FU97, and 293T-CLDN/miR-122 cells infected with HCVcc at an MOI of 1 were determined by a focus-forming assay at 72 h postinfection (bar graph). (B) Exogenous expression of miR-122 in Huh7, JHH-4, and FU97 cells by lentiviral vector (bar graph). Total cellular miRNA extracted from the cells was subjected to qRT-PCR. U6 was used as an internal control. Intracellular HCV RNA in Huh7, JHH-4, and FU97 cells inoculated with HCVcc at an MOI of 1 was determined by qRT-PCR at 12, 24, 48, and 72 h postinfection. Solid and broken lines indicate HCV RNA abundances in miR-122-expressing and GFP-expressing control cells, respectively. (C) Huh7, JHH-4, and FU97 cells were infected with HCVcc at an MOI of 1, fixed with 4% PFA, and subjected to immunofluorescence analyses by using antibodies against core, NS5A, dsRNA, and calregulin. Lipid droplets and cell nuclei were stained by BODIPY and DAPI, respectively. Asterisks indicate significant differences (*, $P < 0.05$; **, $P < 0.01$) versus the results for control cells.

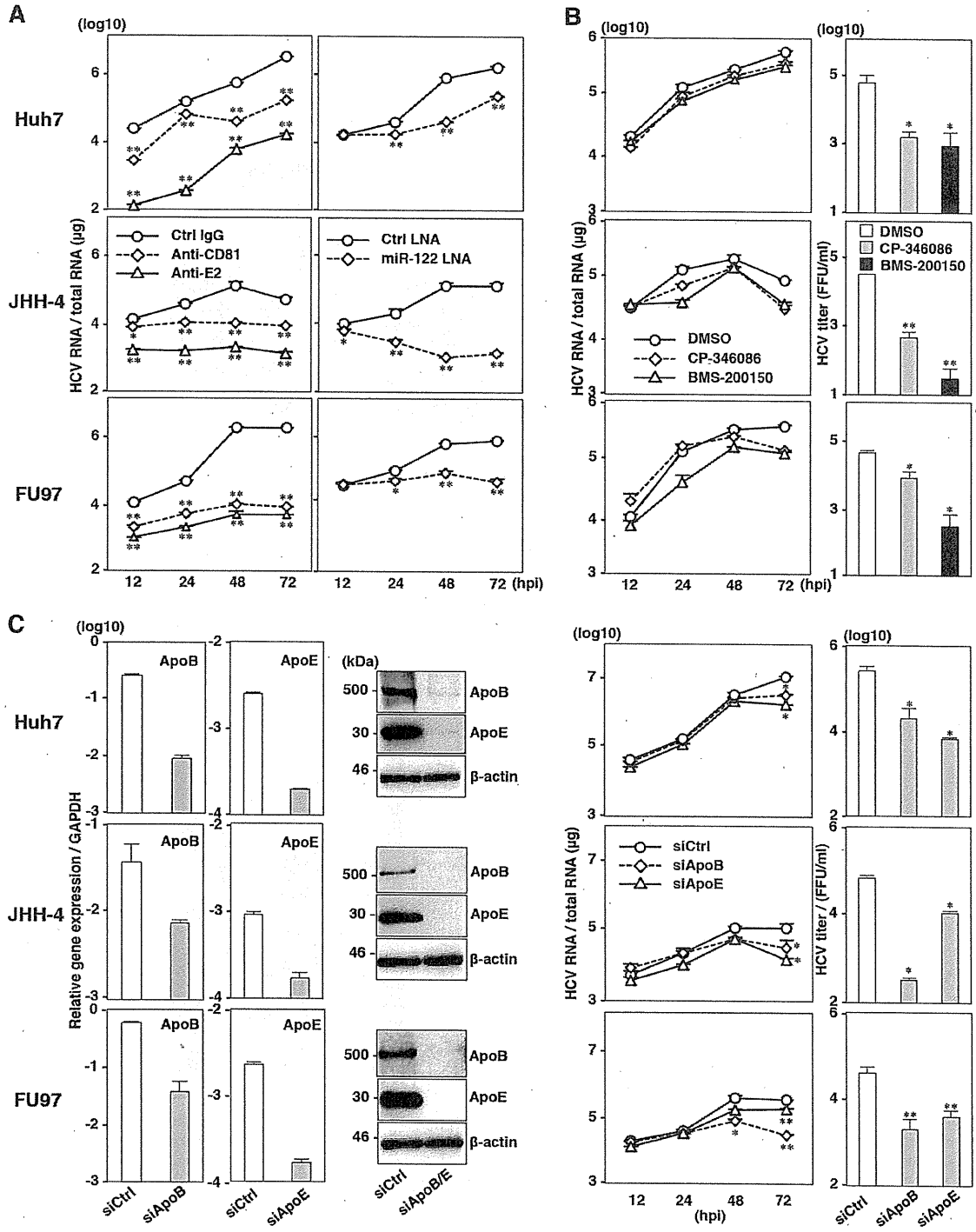

FIG 3 JHH-4 and FU97 cells permit complete propagation of HCVcc without any exogenous expression of host factors crucial for propagation of HCVcc. (A) Effect of inhibitors on the propagation of HCVcc in Huh7, JHH-4, and FU97 cells. (Left panels) HCVcc was preincubated with anti-E2 antibody and inoculated into cells. Cells were preincubated with anti-hCD81 antibody or isotype control antibody (Ctrl IgG) and then infected with HCVcc. (Right panels) Cells were infected with HCVcc and treated with miR-122-LNA (30 nM) or Ctrl-LNA (30 nM) at 6 h postinfection. (B) Huh7, JHH-4, and FU97 cells infected with HCVcc at an MOI of 1 were treated with dimethyl sulfoxide (DMSO) or MTTP inhibitor, CP-346086 (5 μM)or BMS-200150 (10 μM), at 3 h postinfection. Intracellular HCV RNA in cells at 12, 24, 48, and 72 h postinfection was determined by qRT-PCR (left panels). Infectious titers in the culture supernatants of cells infected with HCVcc at an MOI of 1 and treated with 5 μM CP-346086, 10 μM BMS-200150, or dimethyl sulfoxide alone (DMSO) at 3 h postinfection were determined at 72 h postinfection by a focus-forming assay (right graphs). (C) mRNA and protein expression levels of ApoB and ApoE (left panels) in Huh7, JHH-4, and FU97 cells at 48 h posttransfection with siRNA targeting either ApoB or ApoE or a control siRNA (siApoB, siApoE, or siCtrl, respectively) were determined by qRT-PCR and immunoblotting, respectively. Huh7, JHH-4, and FU97 cells were infected with HCVcc at an MOI of 1 at 6 h posttransfection with siRNA targeting either ApoB or ApoE or a control siRNA (siApoB, siApoE, or siCtrl, respectively) (right panels). Intracellular HCV RNA at 12, 24, 48, and 72 h postinfection and infectious titers in the culture supernatants at 72 h postinfection were determined by qRT-PCR and focus-forming assay, respectively. Asterisks indicate significant differences (*, $P < 0.05$; **, $P < 0.01$) versus the results for control cells.

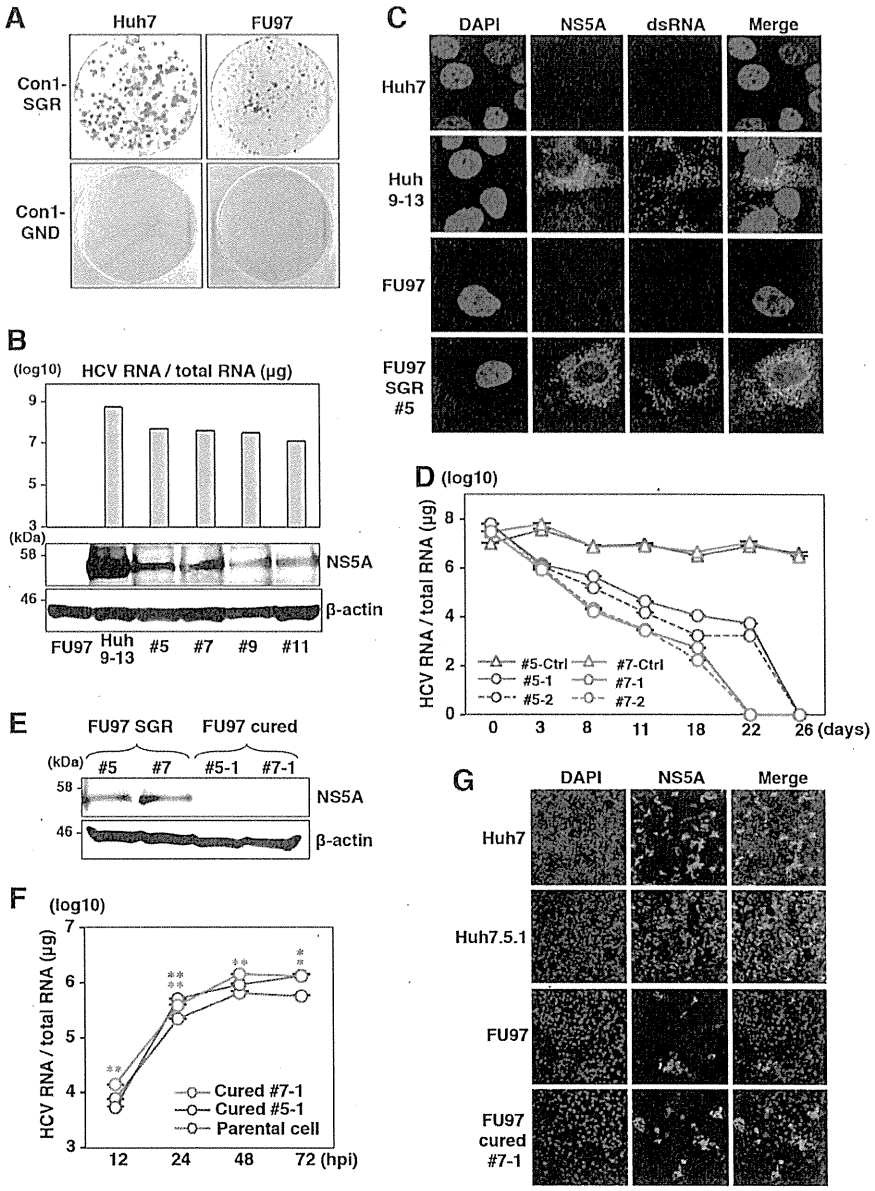

FIG 4 Establishment of HCV RNA replicon and cured FU97 cells. (A) Wild-type SGR RNA (Con1-SGR) or replication-defective RNA (Con1-GND) of the HCV Con1 strain was electroporated into Huh7 and FU97 cells and replaced with medium containing 1 mg/ml and 400 μg/ml of G418 at 24 h postelectroporation, respectively. Colonies were stained with crystal violet at 30 days postselection. (B) Four clones derived from FU97 SGR cells (clones 5, 7, 9, and 11) were subjected to qRT-PCR after extraction of total RNA (upper panel) and to immunoblotting using anti-NS5A antibody (lower panel). Huh9-13 cells, which were Huh7-derived Con1-SGR cells, were used as a positive control. (C) Huh9-13 cells, Huh7 parental cells, FU97-derived Con1-SGR cells (FU97 SGR, clone 5), and FU97 parental cells were fixed in 4% PFA and subjected to immunofluorescence assay using anti-NS5A and anti-dsRNA antibodies. Cell nuclei were stained by DAPI. (D) Elimination of HCV RNA from FU97-derived Con1-SGR cells. Two clones derived from FU97 SGR cells (clones 5 and 7) were treated with a combination of either 100 IU/ml of IFN-α and 100 nM BILN 2061 (clones 5-1 and 7-1) or 10 pM of BMS-790052 and 100 nM BILN 2061 (clones 5-2 and 7-2) to eliminate the HCV genome. Clones 5-Ctrl and 7-Ctrl are negative controls, untreated with anti-HCV drugs. Intracellular HCV RNA at 3, 8, 11, 18, 22, and 26 days posttreatment was determined by qRT-PCR. (E) The expression levels of NS5A in FU97 SGR cells (clones 5 and 7) and in FU97 cured cells (clones 5-1 and 7-1) were determined by immunoblot analysis using anti-NS5A antibody. (F) FU97 cured cells (clone 5-1 and clone 7-1) and parental cells were infected with HCVcc at an MOI of 1; the levels of intracellular HCV RNA at 12, 24, 48, and 72 h postinfection were determined by qRT-PCR. (G) The expression of NS5A in Huh7, Huh7.5.1, FU97, and cured FU97 clone 7-1 was determined by immunofluorescence analysis at 72 h postinfection by using anti-NS5A antibody. Asterisks indicate significant differences (*, $P < 0.05$; **, $P < 0.01$) versus the results for control cells.

recently (15). To clarify the pathogenesis of HCV depending on the genotypes, the establishment of cell-culture-adapted clones derived from various genotypes is essential (58). Viable JFH1-based intergenotypic recombinants, containing genotype-specific structural proteins, p7 and the complete or partial NS2, were generated for various genotypes of HCV (56, 59, 60). Although robust propagation systems of full-length HCV infectious clones of the H77 strain (genotype 1a) (61), TN strain (1a) (62), JFH-2 strain

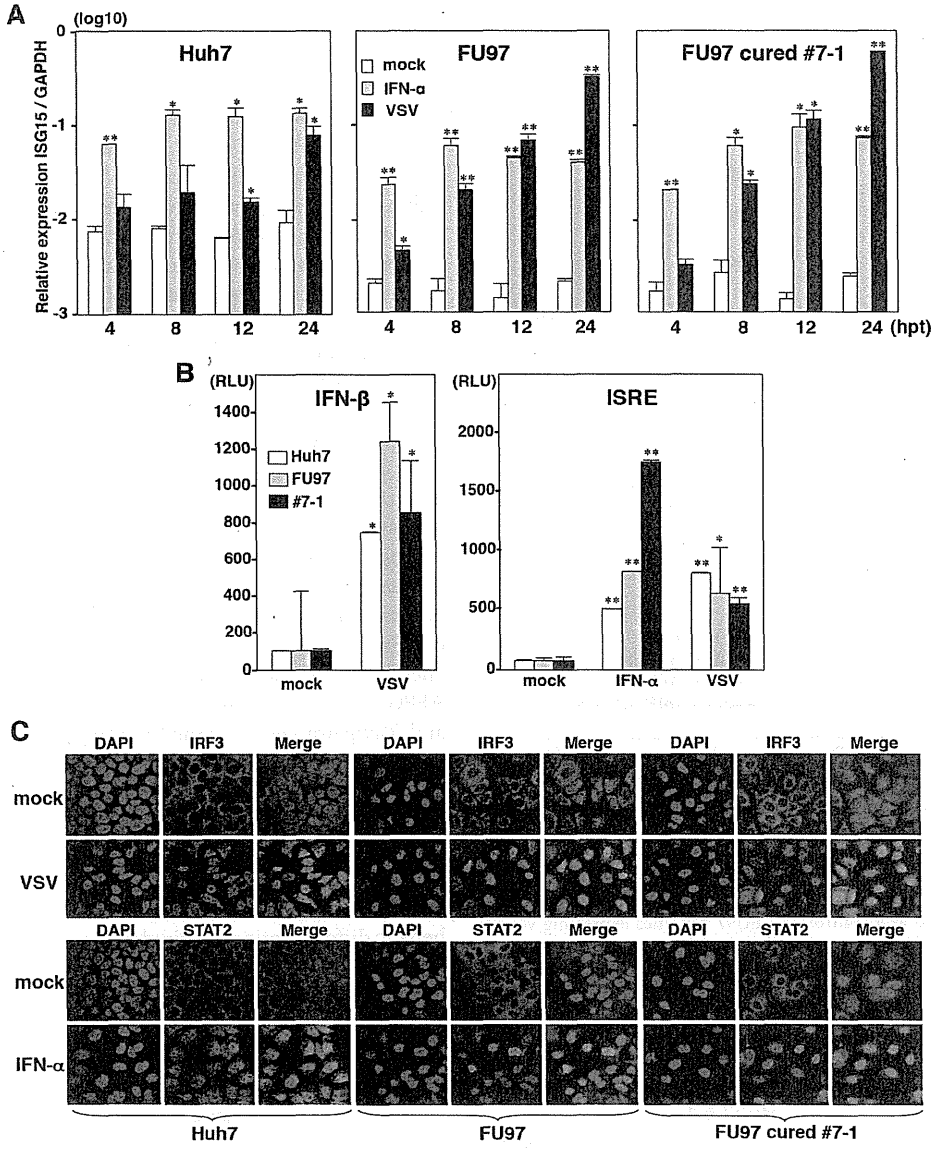

FIG 5 Innate immune response in cured FU97 cells. (A) Huh7, parental, and cured FU97 cells (clone 7-1) were stimulated with 100 IU/ml of IFN-α or infected with VSV. The expression of mRNA of ISG15 at 4, 8, 12, and 24 h posttreatment (hpt) was determined by qPCR and standardized by that of glyceraldehyde-3-phosphate dehydrogenase (GAPDH). (B) Huh7, parental FU97, and cured FU97 (clone 7-1) cells cotransfected with pIFN-β-Luc and pRL-SV40 were infected with VSV at an MOI of 1 at 24 h posttransfection (left). Cells cotransfected with pISRE-Luc and pRL-SV40 were infected with VSV at an MOI of 1 or stimulated with 100 IU/ml of IFN-α at 24 h posttransfection (right). Luciferase activities were determined at 24 h posttreatment. (C) Huh7, parental FU97, and cured FU97 (clone 7-1) cells were infected with VSV at an MOI of 1 or stimulated with 100 IU/ml of IFN-α, fixed with 4% PFA at 18 h posttreatment, and subjected to immunofluorescence assay using anti-IRF3 and -STAT2 antibodies. Cell nuclei were stained by DAPI. Asterisks indicate significant differences (*, $P < 0.05$; **, $P < 0.01$) from the results for control cells.

(2a) (34), and S310 strain (3a) (63) were established, the construction of infectious clones of other genotypes has not succeeded yet.

Because permissive cell lines for HCVcc infection *in vitro* had been limited to Huh7 cells due to cell tropism and the narrow host range (13, 14), the establishment of a novel cell culture system supporting HCV propagation is needed for further HCV analyses. Previous reports have demonstrated that HepG2, Hep3B, and HEK293 cells permit HCVcc propagation (16, 17, 64). However, exogenous expression of host factors is necessary for complete propagation of HCVcc in these cell lines. In HepG2 and Hep3B cells, overexpression of miR-122 is essential for efficient replication of HCV RNA (16, 17). In HEK293 cells, the exogenous expression of CLDN1, miR-122, and ApoE was required for infectious particle formation upon infection with HCVcc (64). On the other hand, JHH-4 and FU97 cells permit complete propagation of HCVcc without any exogenous expression of the host factors required for propagation of HCVcc. JHH-4 cells grown in a three-dimensional radial-flow bioreactor were successfully infected following inoculation with plasma from an HCV carrier and transfection of HCV RNA transcribed from full-length cDNA (44). In

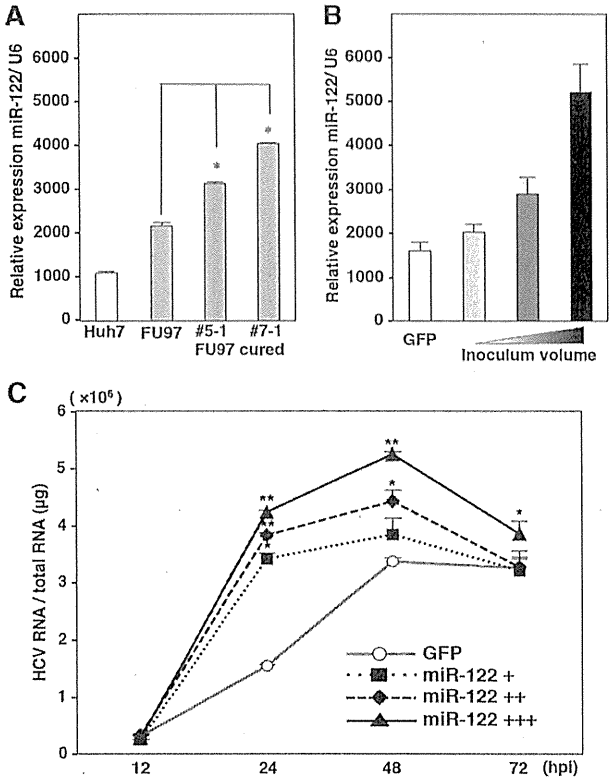

FIG 6 Expression of miR-122 is one of the determinants for HCV RNA abundances. (A) Total RNA was extracted from Huh7 and parental and cured FU97 (clones 5-1 and 7-1) cells, and the relative expression of miR-122 was determined by qPCR. U6 snRNA was used as an internal control. (B) Establishment of FU97 cell lines stably expressing various concentration of miR-122 by infection with a lentiviral vector. FU97 cells infected with lentiviral vector to express GFP were used as a control. (C) FU97 cell lines expressing various concentrations of miR-122 were infected with HCVcc at an MOI of 1, and HCV RNA abundances were determined at 12, 24, 48, and 72 h postinfection (hpi) by qRT-PCR. Asterisks indicate significant differences (*, $P < 0.05$; **, $P < 0.01$) versus the results for control cells.

addition, JHH-4 cells were suggested to possess some host factors involved in the enhanced translation of HCV RNA (64, 65). Furthermore, high susceptibility of FU97 cells to HCVcc/JFH-2 infection compared to Huh7 cells raises the possibility of using FU97 cells for the propagation of HCVcc derived from other genotypes, including the H77, TN, and S310 strains.

AFP-producing gastric cancer (AFPGC) cell lines, FU97 and Takigawa cells (66), which were identified by using a cDNA array database, were shown to express high levels of liver-specific factors. AFPGC is a rare case and exhibits a worse prognosis and the characteristics of early hepatic metastasis (67). It is hypothesized that production of AFP, which is suppressed in mature hepatocytes, is induced in HCC by the dedifferentiation of cancer cells or the increase in oval cells in the oncogenic pathway (68). Oval cells are believed to be capable of producing AFP, are candidates for hepatic stem cells, have bipotentiality to differentiate into hepatocytes and bile duct epithelial cells, and play an important role in liver regeneration (69, 70). These hypotheses suggest that cancer cells acquired a new function, such as the ability to produce AFP through an alteration in differentiation status. Although the mechanism of AFP production in gastric cancer remains unknown, hepatic dedifferentiation might be induced in gastric cancer. Furthermore, previous reports have proposed the concept of "hepatoid adenocarcinoma" based on the differentiation of AFPGC into hepatocyte-like cells (71, 72), suggesting that FU97 and Takigawa cells obtained the hepatocyte-like characteristics required for HCV propagation through dedifferentiation during the oncogenic process. In addition, recent studies demonstrated that hepatocyte-like cells derived from induced pluripotent stem cells (iPS cells/iPSCs) express high levels of miR-122 and VLDL-associated proteins and support propagation of HCVcc and HCV derived from patient serum (28–30). These results suggest that hepatic differentiation required for hepatic functions plays crucial roles in HCV propagation. In accord with these observations, our data suggest that cancer cell lines differentiated into hepatocyte-

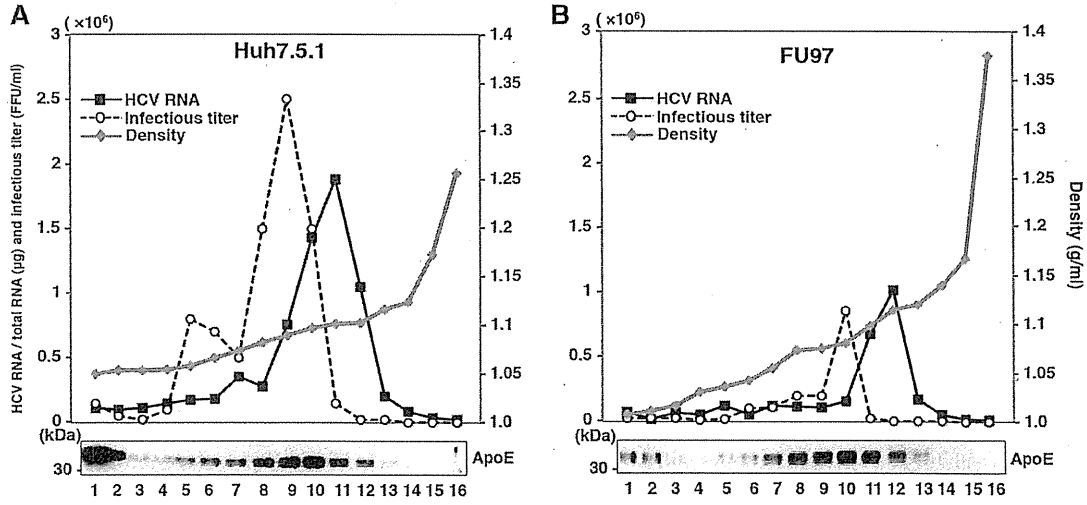

FIG 7 HCV particles produced in FU97 cells exhibit similar characteristics to those in hepatic cells. HCV particles in the culture supernatants of Huh7.5.1 and FU97 cells were harvested at 72 h postinfection with HCVcc and analyzed by using iodixanol density gradient centrifugation. HCV RNA and infectious titers of each fraction were determined by qRT-PCR and focus-forming assay, respectively. Buoyant density was plotted for each fraction (upper panels). Expression of ApoE in each fraction was detected by immunoblotting using anti-ApoE antibody (lower panels).

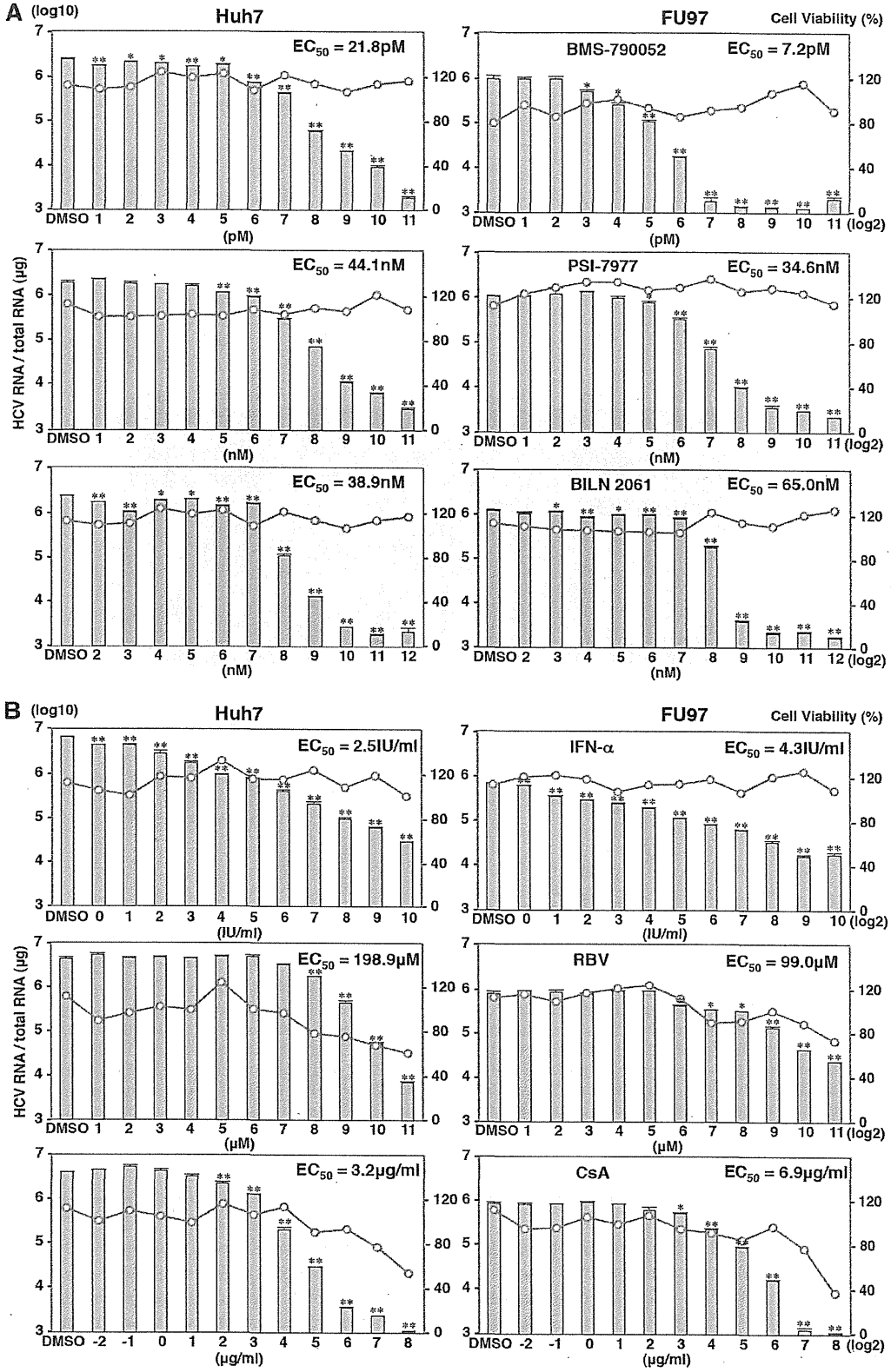

FIG 8 Effects of anti-HCV drugs on the propagation of HCVcc in FU97 cells. (A) Effect of DAAs on the propagation of HCVcc in Huh7 and FU97 cells. Cells infected with HCVcc at an MOI of 1 were treated with BMS-790052, PSI-7977, and BILN 2061 at 3 h postinfection (identifications in right-hand panels). (B) Effect of HCV inhibitors targeting host factors on the propagation of HCVcc in Huh7 and FU97 cells. Cells infected with HCVcc at an MOI of 1 were treated with IFN-α, RBV (middle), and cyclosporine (CsA) at 3 h postinfection (identifications in right-hand panels). Intracellular HCV RNA levels were determined by qRT-PCR at 48 h postinfection (bar graphs), and cell viability was determined as a percentage of the viability of cells treated with 0.1% dimethyl sulfoxide (DMSO) at 48 h posttreatment (line graphs). From the assay results, the 50% effective concentration (EC_{50}) of each reagent was determined. Asterisks indicate significant differences (*, $P < 0.05$; **, $P < 0.01$) versus the results for control cells.

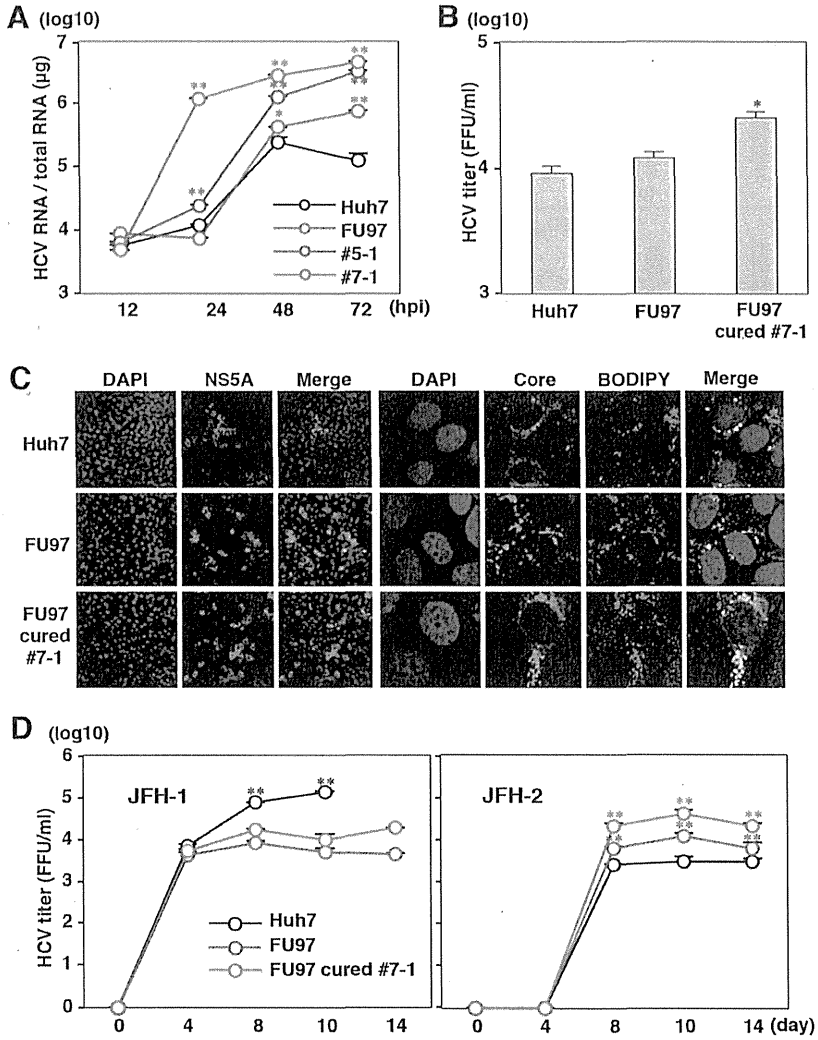

FIG 9 Propagation of HCVcc/JFH-2 in FU97 cells. (A) Huh7, FU97 parental, FU97 cured 5-1, and FU97 cured 7-1 cells were infected with HCVcc/JFH-2 at an MOI of 1, and the intracellular HCV RNA level was determined by qRT-PCR at 12, 24, 48, and 72 h postinfection. (B) Huh7, FU97, and FU97 cured 7-1 cells were infected with HCVcc/JFH-2 at an MOI of 1, and infectious titers in the culture supernatants were determined by focus-forming assay. (C) Huh7, FU97, and FU97 cured 7-1 cells were infected with HCVcc/JFH-2 at an MOI of 1, fixed with 4% PFA at 72 h postinfection, and subjected to immunofluorescence assay using antibodies against NS5A or core. Lipid droplets and cell nuclei were stained with BODIPY and DAPI, respectively. (D) *In vitro*-transcribed JFH-1 and JFH-2 RNAs were electroporated into Huh7, FU97, and FU97 cured 7-1 cells. The infectious titers of JFH-1 and JFH-2 in the culture supernatants from these cells were determined by focus-forming assay up to 14 days postransduction. Asterisks indicate significant differences (*, $P < 0.05$; **, $P < 0.01$) versus the results for control cells.

like cells to gain hepatic functions could permit complete propagation of HCVcc.

Treatment with DAAs including BMS-790052 (NS5A inhibitor) (73), PSI-7977 (NS5B polymerase inhibitor) (74), and BILN 2061 (NS3/4A protease inhibitor) (75) inhibited propagation of HCV in both Huh7 and FU97 cells infected with HCVcc without any cell toxicity. Antiviral effects of BMS-790052 and BILN 2061 were significantly different between Huh7 and FU97 cells, suggesting that efficacies of DAAs are varied, depending on cell lines. Although anti-HCV drugs targeting host factors including IFN-α, RBV, and cyclosporine also inhibited propagation of HCVcc in a dose-dependent manner in both Huh7 and FU97 cells, treatment with RBV and cyclosporine produced cell toxicity at higher concentrations than treatment with DAAs. Although the antiviral mechanism of RBV against HCV has not been well elucidated yet (53), inhibitory effects of RBV against HCV infection were significantly higher in Li23 cells than those in Huh7 cells (76, 77), and RBV also exhibited a low inhibitory effect upon infection with HCVcc in Huh7 cells compared to that in FU97 cells. Although adenosine kinase (ADK) was shown to be a determinant for the sensitivity of RBV (78), the expression levels of ADK in Huh7 and FU97 cell lines were comparable (data not shown).

The *IL28B* genotype is associated with the sensitivity of IFN treatment for chronic hepatitis C patients (79–81), and patients with the minor *IL28B* genotype exhibit lower susceptibility to the treatment than those with major genotypes. Although FU97 cells showed lower sensitivity to the IFN-α treatment than Huh7 cells, FU97 and Huh7 cells possess major and minor *IL28B* genotypes

(data not shown), respectively. Furthermore, induction of ISG15 by treatment with IFN-α was almost comparable between Huh7 and FU97 cells (Fig. 5A), and expression levels of IFN-α receptor in the cell lines were the same (data not shown), suggesting the involvement of other factors in the difference in the IFN responses between FU97 and Huh7 cells.

Cyclophilins possess peptidyl-prolyl *cis/trans* isomerase (PPIase) activity and are involved in protein folding and assembly. Cyclophilin A (CypA), the most abundant cyclophilin, localizes in the cytoplasm and interacts with the immunosuppressive drug cyclosporine (82). In addition, CypA has been shown to be involved in the propagation of human immunodeficiency virus (83, 84), hepatitis B virus (85, 86), influenza A virus (87), and HCV (88). Replication of HCV RNA was inhibited by suppression of the PPIase activity of CypA by treatments with cyclosporine, mutation in the active site of CypA, and knockdown of CypA (55, 89–91). The same level of CypA expression in Huh7 and FU97 cells (data not shown) suggests that the difference in inhibitory effect of cyclosporine in the cell lines may be attributable to other reasons, such as a difference in PPIase activity of CypA in these cell lines. The differences in the efficacy of anti-HCV drugs between Huh7 and FU97 cells were small; however, FU97 cells have the possibility to possess antiviral activity different from that of Huh7 cells.

In summary, we identified novel permissive cell lines for complete propagation of HCVcc without any artificial manipulation. In particular, gastric cancer-derived FU97 cells exhibited a much higher susceptibility to HCVcc/JFH-2 infection than observed in Huh7 cells, suggesting that FU97 cells would be useful for further investigation of the HCV life cycle, as well as the development of therapeutic agents for chronic hepatitis C.

ACKNOWLEDGMENTS

We thank M. Tomiyama for her secretarial work and M. Ishibashi and Y. Sugiyama for their technical assistance. We also thank M. Hijikata, R. Bartenschlager, S. Akira, F. Chisari, and M. Whitt for providing experimental materials.

This work was supported in part by grants-in-aid from the Japanese Ministry of Health, Labor, and Welfare (Research on Hepatitis), the Japanese Ministry of Education, Culture, Sports, Science, and Technology, the Naito Foundation, and the Takeda Science Foundation.

REFERENCES

1. **Maasoumy B, Wedemeyer H.** 2012. Natural history of acute and chronic hepatitis C. Best Pract. Res. Clin. Gastroenterol. **26**:401–412. http://dx.doi.org/10.1016/j.bpg.2012.09.009.
2. **Poynard T, Colombo M, Bruix J, Schiff E, Terg R, Flamm S, Moreno-Otero R, Carrilho F, Schmidt W, Berg T, McGarrity T, Heathcote EJ, Gonçales F, Diago M, Craxi A, Silva M, Bedossa P, Mukhopadhyay P, Griffel L, Burroughs M, Brass C, Albrecht J, Epic Study Group.** 2009. Peginterferon alfa-2b and ribavirin: effective in patients with hepatitis C who failed interferon alfa/ribavirin therapy. Gastroenterology **136**:1618–1628.e2. http://dx.doi.org/10.1053/j.gastro.2009.01.039.
3. **Chatel-Chaix L, Germain MA, Götte M, Lamarre D.** 2012. Direct-acting and host-targeting HCV inhibitors: current and future directions. Curr. Opin. Virol. **2**:588–598. http://dx.doi.org/10.1016/j.coviro.2012.08.002.
4. **Jazwinski AB, Muir AJ.** 2011. Direct-acting antiviral medications for chronic hepatitis C virus infection. Gastroenterol. Hepatol. (NY) **7**:154–162. http://www.ncbi.nlm.nih.gov/pmc/articles/PMC3079144/.
5. **McHutchison JG, Manns MP, Muir AJ, Terrault NA, Jacobson IM, Afdhal NH, Heathcote EJ, Zeuzem S, Reesink HW, Garg J, Bsharat M, George S, Kauffman RS, Adda N, Di Bisceglie AM, Team PS.** 2010. Telaprevir for previously treated chronic HCV infection. N. Engl. J. Med. **362**:1292–1303. http://dx.doi.org/10.1056/NEJMoa0908014.
6. **Lok AS, Gardiner DF, Lawitz E, Martorell C, Everson GT, Ghalib R, Reindollar R, Rustgi V, McPhee F, Wind-Rotolo M, Persson A, Zhu K, Dimitrova DI, Eley T, Guo T, Grasela DM, Pasquinelli C.** 2012. Preliminary study of two antiviral agents for hepatitis C genotype 1. N. Engl. J. Med. **366**:216–224. http://dx.doi.org/10.1056/NEJMoa1104430.
7. **McPhee F, Friborg J, Levine S, Chen C, Falk P, Yu F, Hernandez D, Lee MS, Chaniewski S, Sheaffer AK, Pasquinelli C.** 2012. Resistance analysis of the hepatitis C virus NS3 protease inhibitor asunaprevir. Antimicrob. Agents Chemother. **56**:3670–3681. http://dx.doi.org/10.1128/AAC.00308-12.
8. **Pelosi LA, Voss S, Liu M, Gao M, Lemm JA.** 2012. Effect on hepatitis C virus replication of combinations of direct-acting antivirals, including NS5A inhibitor daclatasvir. Antimicrob. Agents Chemother. **56**:5230–5239. http://dx.doi.org/10.1128/AAC.01209-12.
9. **Fridell RA, Wang C, Sun JH, O'Boyle DR, Nower P, Valera L, Qiu D, Roberts S, Huang X, Kienzle B, Bifano M, Nettles RE, Gao M.** 2011. Genotypic and phenotypic analysis of variants resistant to hepatitis C virus nonstructural protein 5A replication complex inhibitor BMS-790052 in humans: in vitro and in vivo correlations. Hepatology **54**:1924–1935. http://dx.doi.org/10.1002/hep.24594.
10. **Sarrazin C, Zeuzem S.** 2010. Resistance to direct antiviral agents in patients with hepatitis C virus infection. Gastroenterology **138**:447–462. http://dx.doi.org/10.1053/j.gastro.2009.11.055.
11. **Susser S, Welsch C, Wang Y, Zettler M, Domingues FS, Karey U, Hughes E, Ralston R, Tong X, Herrmann E, Zeuzem S, Sarrazin C.** 2009. Characterization of resistance to the protease inhibitor boceprevir in hepatitis C virus-infected patients. Hepatology **50**:1709–1718. http://dx.doi.org/10.1002/hep.23192.
12. **Vermehren J, Sarrazin C.** 2012. The role of resistance in HCV treatment. Best Pract. Res. Clin. Gastroenterol. **26**:487–503. http://dx.doi.org/10.1016/j.bpg.2012.09.011.
13. **Bukh J.** 2004. A critical role for the chimpanzee model in the study of hepatitis C. Hepatology **39**:1469–1475. http://dx.doi.org/10.1002/hep.20268.
14. **Bukh J.** 2012. Animal models for the study of hepatitis C virus infection and related liver disease. Gastroenterology **142**:1279–1287.e1273. http://dx.doi.org/10.1053/j.gastro.2012.02.016.
15. **Wakita T, Pietschmann T, Kato T, Date T, Miyamoto M, Zhao Z, Murthy K, Habermann A, Kräusslich HG, Mizokami M, Bartenschlager R, Liang TJ.** 2005. Production of infectious hepatitis C virus in tissue culture from a cloned viral genome. Nat. Med. **11**:791–796. http://dx.doi.org/10.1038/nm1268.
16. **Narbus CM, Israelow B, Sourisseau M, Michta ML, Hopcraft SE, Zeiner GM, Evans MJ.** 2011. HepG2 cells expressing microRNA miR-122 support the entire hepatitis C virus life cycle. J. Virol. **85**:12087–12092. http://dx.doi.org/10.1128/JVI.05843-11.
17. **Kambara H, Fukuhara T, Shiokawa M, Ono C, Ohara Y, Kamitani W, Matsuura Y.** 2012. Establishment of a novel permissive cell line for the propagation of hepatitis C virus by expression of microRNA miR122. J. Virol. **86**:1382–1393. http://dx.doi.org/10.1128/JVI.06242-11.
18. **Fukuhara T, Kambara H, Shiokawa M, Ono C, Katoh H, Morita E, Okuzaki D, Maehara Y, Koike K, Matsuura Y.** 2012. Expression of microRNA miR-122 facilitates an efficient replication in nonhepatic cells upon infection with hepatitis C virus. J. Virol. **86**:7918–7933. http://dx.doi.org/10.1128/JVI.00567-12.
19. **Chang KS, Jiang J, Cai Z, Luo G.** 2007. Human apolipoprotein E is required for infectivity and production of hepatitis C virus in cell culture. J. Virol. **81**:13783–13793. http://dx.doi.org/10.1128/JVI.01091-07.
20. **Gastaminza P, Cheng G, Wieland S, Zhong J, Liao W, Chisari FV.** 2008. Cellular determinants of hepatitis C virus assembly, maturation, degradation, and secretion. J. Virol. **82**:2120–2129. http://dx.doi.org/10.1128/JVI.02053-07.
21. **Huang H, Sun F, Owen DM, Li W, Chen Y, Gale M, Ye J.** 2007. Hepatitis C virus production by human hepatocytes dependent on assembly and secretion of very low-density lipoproteins. Proc. Natl. Acad. Sci. U. S. A. **104**:5848–5853. http://dx.doi.org/10.1073/pnas.0700760104.
22. **Jiang J, Luo G.** 2009. Apolipoprotein E but not B is required for the formation of infectious hepatitis C virus particles. J. Virol. **83**:12680–12691. http://dx.doi.org/10.1128/JVI.01476-09.
23. **Syed GH, Amako Y, Siddiqui A.** 2010. Hepatitis C virus hijacks host lipid metabolism. Trends Endocrinol. Metab. **21**:33–40. http://dx.doi.org/10.1016/j.tem.2009.07.005.
24. **Miyanari Y, Atsuzawa K, Usuda N, Watashi K, Hishiki T, Zayas M, Bartenschlager R, Wakita T, Hijikata M, Shimotohno K.** 2007. The lipid

droplet is an important organelle for hepatitis C virus production. Nat. Cell Bjol. 9:1089–1097. http://dx.doi.org/10.1038/ncb1631.
25. Jögi A, Vaapil M, Johansson M, Påhlman S. 2012. Cancer cell differentiation heterogeneity and aggressive behavior in solid tumors. Ups. J. Med. Sci. 117:217–224. http://dx.doi.org/10.3109/03009734.2012.659294.
26. Nakabayashi H, Taketa K, Miyano K, Yamane T, Sato J. 1982. Growth of human hepatoma cells lines with differentiated functions in chemically defined medium. Cancer Res. 42:3858–3863.
27. Slany A, Haudek VJ, Zwickl H, Gundacker NC, Grusch M, Weiss TS, Seir K, Rodgarkia-Dara C, Hellerbrand C, Gerner C. 2010. Cell characterization by proteome profiling applied to primary hepatocytes and hepatocyte cell lines Hep-G2 and Hep-3B. J. Proteome Res. 9:6–21. http://dx.doi.org/10.1021/pr900057t.
28. Schwartz RE, Trehan K, Andrus L, Sheahan TP, Ploss A, Duncan SA, Rice CM, Bhatia SN. 2012. Modeling hepatitis C virus infection using human induced pluripotent stem cells. Proc. Natl. Acad. Sci. U. S. A. 109:2544–2548. http://dx.doi.org/10.1073/pnas.1121400109.
29. Si-Tayeb K, Noto FK, Nagaoka M, Li J, Battle MA, Duris C, North PE, Dalton S, Duncan SA. 2010. Highly efficient generation of human hepatocyte-like cells from induced pluripotent stem cells. Hepatology 51:297–305. http://dx.doi.org/10.1002/hep.23354.
30. Wu X, Robotham JM, Lee E, Dalton S, Kneteman NM, Gilbert DM, Tang H. 2012. Productive hepatitis C virus infection of stem cell-derived hepatocytes reveals a critical transition to viral permissiveness during differentiation. PLoS Pathog. 8:e1002617. http://dx.doi.org/10.1371/journal.ppat.1002617.
31. Debruyne EN, Delanghe JR. 2008. Diagnosing and monitoring hepatocellular carcinoma with alpha-fetoprotein: new aspects and applications. Clin. Chim. Acta 395:19–26. http://dx.doi.org/10.1016/j.cca.2008.05.010.
32. Kupershmidt I, Su QJ, Grewal A, Sundaresh S, Halperin I, Flynn J, Shekar M, Wang H, Park J, Cui W, Wall GD, Wisotzkey R, Alag S, Akhtari S, Ronaghi M. 2010. Ontology-based meta-analysis of global collections of high-throughput public data. PLoS One 5:e13066. http://dx.doi.org/10.1371/journal.pone.0013066.
33. Masaki T, Suzuki R, Saeed M, Mori K, Matsuda M, Aizaki H, Ishii K, Maki N, Miyamura T, Matsuura Y, Wakita T, Suzuki T. 2010. Production of infectious hepatitis C virus by using RNA polymerase I-mediated transcription. J. Virol. 84:5824–5835. http://dx.doi.org/10.1128/JVI.02397-09.
34. Date T, Kato T, Kato J, Takahashi H, Morikawa K, Akazawa D, Murayama A, Tanaka-Kaneko K, Sata T, Tanaka Y, Mizokami M, Wakita T. 2012. Novel cell culture-adapted genotype 2a hepatitis C virus infectious clone. J. Virol. 86:10805–10820. http://dx.doi.org/10.1128/JVI.07235-11.
35. Pietschmann T, Lohmann V, Kaul A, Krieger N, Rinck G, Rutter G, Strand D, Bartenschlager R. 2002. Persistent and transient replication of full-length hepatitis C virus genomes in cell culture. J. Virol. 76:4008–4021. http://dx.doi.org/10.1128/JVI.76.8.4008-4021.2002.
36. Tani H, Komoda Y, Matsuo E, Suzuki K, Hamamoto I, Yamashita T, Moriishi K, Fujiyama K, Kanto T, Hayashi N, Owsianka A, Patel AH, Whitt MA, Matsuura Y. 2007. Replication-competent recombinant vesicular stomatitis virus encoding hepatitis C virus envelope proteins. J. Virol. 81:8601–8612. http://dx.doi.org/10.1128/JVI.00608-07.
37. Moriishi K, Shoji I, Mori Y, Suzuki R, Suzuki T, Kataoka C, Matsuura Y. 2010. Involvement of PA28γ in the propagation of hepatitis C virus. Hepatology 52:411–420. http://dx.doi.org/10.1002/hep.23680.
38. Fukuhara T, Tani H, Shiokawa M, Goto Y, Abe T, Taketomi A, Shirabe K, Maehara Y, Matsuura Y. 2011. Intracellular delivery of serum-derived hepatitis C virus. Microbes Infect. 13:405–412. http://dx.doi.org/10.1016/j.micinf.2011.01.005.
39. Morris T, Robertson B, Gallagher M. 1996. Rapid reverse transcription-PCR detection of hepatitis C virus RNA in serum by using the TaqMan fluorogenic detection system. J. Clin. Microbiol. 34:2933–2936.
40. Latchman DS, Brzeski H, Lovell-Badge R, Evans MJ. 1984. Expression of the alpha-fetoprotein gene in pluripotent and committed cells. Biochim. Biophys. Acta 783:130–136. http://dx.doi.org/10.1016/0167-4781(84)90004-6.
41. Roelandt P, Obeid S, Paeshuyse J, Vanhove J, Van Lommel A, Nahmias Y, Nevens F, Neyts J, Verfaillie CM. 2012. Human pluripotent stem cell-derived hepatocytes support complete replication of hepatitis C virus. J. Hepatol. 57:246–251. http://dx.doi.org/10.1016/j.jhep.2012.03.030.
42. Mee CJ, Grove J, Harris HJ, Hu K, Balfe P, McKeating JA. 2008. Effect of cell polarization on hepatitis C virus entry. J. Virol. 82:461–470. http://dx.doi.org/10.1128/JVI.01894-07.
43. Wilson GK, Stamataki Z. 2012. In vitro systems for the study of hepatitis C virus infection. Int. J. Hepatol. 2012:292591. http://dx.doi.org/10.1155/2012/292591.
44. Aizaki H, Nagamori S, Matsuda M, Kawakami H, Hashimoto O, Ishiko H, Kawada M, Matsuura T, Hasumura S, Matsuura Y, Suzuki T, Miyamura T. 2003. Production and release of infectious hepatitis C virus from human liver cell cultures in the three-dimensional radial-flow bioreactor. Virology 314:16–25. http://dx.doi.org/10.1016/S0042-6822(03)00383-0.
45. Pileri P, Uematsu Y, Campagnoli S, Galli G, Falugi F, Petracca R, Weiner AJ, Houghton M, Rosa D, Grandi G, Abrignani S. 1998. Binding of hepatitis C virus to CD81. Science 282:938–941. http://dx.doi.org/10.1126/science.282.5390.938.
46. Scarselli E, Ansuini H, Cerino R, Roccasecca RM, Acali S, Filocamo G, Traboni C, Nicosia A, Cortese R, Vitelli A. 2002. The human scavenger receptor class B type I is a novel candidate receptor for the hepatitis C virus. EMBO J. 21:5017–5025. http://dx.doi.org/10.1093/emboj/cdf529.
47. Evans MJ, von Hahn T, Tscherne DM, Syder AJ, Panis M, Wölk B, Hatziioannou T, McKeating JA, Bieniasz PD, Rice CM. 2007. Claudin-1 is a hepatitis C virus co-receptor required for a late step in entry. Nature 446:801–805. http://dx.doi.org/10.1038/nature05654.
48. Ploss A, Evans MJ, Gaysinskaya VA, Panis M, You H, de Jong YP, Rice CM. 2009. Human occludin is a hepatitis C virus entry factor required for infection of mouse cells. Nature 457:882–886. http://dx.doi.org/10.1038/nature07684.
49. Blight KJ, McKeating JA, Rice CM. 2002. Highly permissive cell lines for subgenomic and genomic hepatitis C virus RNA replication. J. Virol. 76:13001–13014. http://dx.doi.org/10.1128/JVI.76.24.13001-13014.2002.
50. Sumpter R, Loo YM, Foy E, Li K, Yoneyama M, Fujita T, Lemon SM, Gale M. 2005. Regulating intracellular antiviral defense and permissiveness to hepatitis C virus RNA replication through a cellular RNA helicase, RIG-I. J. Virol. 79:2689–2699. http://dx.doi.org/10.1128/JVI.79.5.2689-2699.2005.
51. Lindenbach BD, Evans MJ, Syder AJ, Wolk B, Tellinghuisen TL, Liu CC, Maruyama T, Hynes RO, Burton DR, McKeating JA, Rice CM. 2005. Complete replication of hepatitis C virus in cell culture. Science 309:623–626. http://dx.doi.org/10.1126/science.1114016.
52. Lindenbach BD, Meuleman P, Ploss A, Vanwolleghem T, Syder AJ, McKeating JA, Lanford RE, Feinstone SM, Major ME, Leroux-Roels G, Rice CM. 2006. Cell culture-grown hepatitis C virus is infectious in vivo and can be recultured in vitro. Proc. Natl. Acad. Sci. U. S. A. 103:3805–3809. http://dx.doi.org/10.1073/pnas.0511218103.
53. Feld JJ, Hoofnagle JH. 2005. Mechanism of action of interferon and ribavirin in treatment of hepatitis C. Nature 436:967–972. http://dx.doi.org/10.1038/nature04082.
54. Frese M, Pietschmann T, Moradpour D, Haller O, Bartenschlager R. 2001. Interferon-alpha inhibits hepatitis C virus subgenomic RNA replication by an MxA-independent pathway. J. Gen. Virol. 82:723–733. http://vir.sgmjournals.org/content/82/4/723.full.
55. Watashi K, Hijikata M, Hosaka M, Yamaji M, Shimotohno K. 2003. Cyclosporin A suppresses replication of hepatitis C virus genome in cultured hepatocytes. Hepatology 38:1282–1288. http://dx.doi.org/10.1053/jhep.2003.50449.
56. Gottwein JM, Scheel TK, Jensen TB, Lademann JB, Prentoe JC, Knudsen ML, Hoegh AM, Bukh J. 2009. Development and characterization of hepatitis C virus genotype 1–7 cell culture systems: role of CD81 and scavenger receptor class B type I and effect of antiviral drugs. Hepatology 49:364–377. http://dx.doi.org/10.1002/hep.22673.
57. Scheel TK, Gottwein JM, Mikkelsen LS, Jensen TB, Bukh J. 2011. Recombinant HCV variants with NS5A from genotypes 1–7 have different sensitivities to an NS5A inhibitor but not interferon-γ. Gastroenterology 140:1032–1042. http://dx.doi.org/10.1053/j.gastro.2010.11.036.
58. Tariq H, Manzoor S, Parvaiz F, Javed F, Fatima K, Qadri I. 2012. An overview: in vitro models of HCV replication in different cell cultures. Infect. Genet. Evol. 12:13–20. http://dx.doi.org/10.1016/j.meegid.2011.10.009.
59. Pietschmann T, Kaul A, Koutsoudakis G, Shavinskaya A, Kallis S, Steinmann E, Abid K, Negro F, Dreux M, Cosset FL, Bartenschlager R. 2006. Construction and characterization of infectious intragenotypic and intergenotypic hepatitis C virus chimeras. Proc. Natl. Acad. Sci. U. S. A. 103:7408–7413. http://dx.doi.org/10.1073/pnas.0504877103.

60. **Yi M, Ma Y, Yates J, Lemon SM.** 2007. Compensatory mutations in E1, p7, NS2, and NS3 enhance yields of cell culture-infectious intergenotypic chimeric hepatitis C virus. J. Virol. **81**:629–638. http://dx.doi.org/10.1128/JVI.01890-06.
61. **Yi M, Villanueva RA, Thomas DL, Wakita T, Lemon SM.** 2006. Production of infectious genotype 1a hepatitis C virus (Hutchinson strain) in cultured human hepatoma cells. Proc. Natl. Acad. Sci. U. S. A. **103**:2310–2315. http://dx.doi.org/10.1073/pnas.0510727103.
62. **Li YP, Ramirez S, Jensen SB, Purcell RH, Gottwein JM, Bukh J.** 2012. Highly efficient full-length hepatitis C virus genotype 1 (strain TN) infectious culture system. Proc. Natl. Acad. Sci. U. S. A. **109**:19757–19762. http://dx.doi.org/10.1073/pnas.1218260109.
63. **Saeed M, Gondeau C, Hmwe S, Yokokawa H, Date T, Suzuki T, Kato T, Maurel P, Wakita T.** 2013. Replication of hepatitis C virus genotype 3a in cultured cells. Gastroenterology **144**:56–58.e57. http://dx.doi.org/10.1053/j.gastro.2012.09.017.
64. **Da Costa D, Turek M, Felmlee DJ, Girardi E, Pfeffer S, Long G, Bartenschlager R, Zeisel MB, Baumert TF.** 2012. Reconstitution of the entire hepatitis C virus life cycle in nonhepatic cells. J. Virol. **86**:11919–11925. http://dx.doi.org/10.1128/JVI.01066-12.
65. **Aoki Y, Aizaki H, Shimoike T, Tani H, Ishii K, Saito I, Matsuura Y, Miyamura T.** 1998. A human liver cell line exhibits efficient translation of HCV RNAs produced by a recombinant adenovirus expressing T7 RNA polymerase. Virology **250**:140–150. http://dx.doi.org/10.1006/viro.1998.9361.
66. **Matsuda M.** 2000. Biological behavior of an alpha-phetoprotein-producing gastric cancer (FU97). J. Nara Med. Assoc. **51**:79–89.
67. **Chun H, Kwon SJ.** 2011. Clinicopathological characteristics of alpha-fetoprotein-producing gastric cancer. J. Gastric Cancer **11**:23–30. http://dx.doi.org/10.5230/jgc.2011.11.1.23.
68. **Dabeva MD, Laconi E, Oren R, Petkov PM, Hurston E, Shafritz DA.** 1998. Liver regeneration and alpha-fetoprotein messenger RNA expression in the retrorsine model for hepatocyte transplantation. Cancer Res. **58**:5825–5834.
69. **Kuhlmann WD, Peschke P.** 2006. Hepatic progenitor cells, stem cells, and AFP expression in models of liver injury. Int. J. Exp. Pathol. **87**:343–359. http://dx.doi.org/10.1111/j.1365-2613.2006.00485.x.
70. **Watanabe H.** 1971. Early appearance of embryonic γ-globulin in rat serum during carcinogenesis with 4-dimethylaminoazobenzene. Cancer Res. **31**:1192–1194.
71. **Ishikura H, Fukasawa Y, Ogasawara K, Natori T, Tsukada Y, Aizawa M.** 1985. An AFP-producing gastric carcinoma with features of hepatic differentiation. A case report. Cancer **56**:840–848.
72. **Ishikura H, Kirimoto K, Shamoto M, Miyamoto Y, Yamagiwa H, Itoh T, Aizawa M.** 1986. Hepatoid adenocarcinomas of the stomach. An analysis of seven cases. Cancer **58**:119–126.
73. **Nettles RE, Gao M, Bifano M, Chung E, Persson A, Marbury TC, Goldwater R, DeMicco MP, Rodriguez-Torres M, Vutikullird A, Fuentes E, Lawitz E, Lopez-Talavera JC, Grasela DM.** 2011. Multiple ascending dose study of BMS-790052, a nonstructural protein 5A replication complex inhibitor, in patients infected with hepatitis C virus genotype 1. Hepatology **54**:1956–1965. http://dx.doi.org/10.1002/hep.24609.
74. **Elfiky AA, Elshemey WM, Gawad WA, Desoky OS.** 2013. Molecular modeling comparison of the performance of NS5b polymerase inhibitor (PSI-7977) on prevalent HCV genotypes. Protein J. **32**:75–80. http://dx.doi.org/10.1007/s10930-013-9462-9.
75. **Hinrichsen H, Benhamou Y, Wedemeyer H, Reiser M, Sentjens RE, Calleja JL, Forns X, Erhardt A, Crönlein J, Chaves RL, Yong CL, Nehmiz G, Steinmann GG.** 2004. Short-term antiviral efficacy of BILN 2061, a hepatitis C virus serine protease inhibitor, in hepatitis C genotype 1 patients. Gastroenterology **127**:1347–1355. http://dx.doi.org/10.1053/j.gastro.2004.08.002.
76. **Kato N, Abe K, Mori K, Ariumi Y, Dansako H, Ikeda M.** 2009. Genetic variability and diversity of intracellular genome-length hepatitis C virus RNA in long-term cell culture. Arch. Virol. **154**:77–85. http://dx.doi.org/10.1007/s00705-008-0282-8.
77. **Mori K, Ikeda M, Ariumi Y, Dansako H, Wakita T, Kato N.** 2011. Mechanism of action of ribavirin in a novel hepatitis C virus replication cell system. Virus Res. **157**:61–70. http://dx.doi.org/10.1016/j.virusres.2011.02.005.
78. **Mori K, Hiraoka O, Ikeda M, Ariumi Y, Hiramoto A, Wataya Y, Kato N.** 2013. Adenosine kinase is a key determinant for the anti-HCV activity of ribavirin. Hepatology **58**:1236–1244. http://dx.doi.org/10.1002/hep.26421.
79. **Fukuhara T, Taketomi A, Motomura T, Okano S, Ninomiya A, Abe T, Uchiyama H, Soejima Y, Shirabe K, Matsuura Y, Maehara Y.** 2010. Variants in *IL28B* in liver recipients and donors correlate with response to peg-interferon and ribavirin therapy for recurrent hepatitis C. Gastroenterology **139**:1577–1585.e3. http://dx.doi.org/10.1053/j.gastro.2010.07.058.
80. **Suppiah V, Moldovan M, Ahlenstiel G, Berg T, Weltman M, Abate ML, Bassendine M, Spengler U, Dore GJ, Powell E, Riordan S, Sheridan D, Smedile A, Fragomeli V, Muller T, Bahlo M, Stewart GJ, Booth DR, George J.** 2009. IL28B is associated with response to chronic hepatitis C interferon-alpha and ribavirin therapy. Nat. Genet. **41**:1100–1104. http://dx.doi.org/10.1038/ng.447.
81. **Tanaka Y, Nishida N, Sugiyama M, Kurosaki M, Matsuura K, Sakamoto N, Nakagawa M, Korenaga M, Hino K, Hige S, Ito Y, Mita E, Tanaka E, Mochida S, Murawaki Y, Honda M, Sakai A, Hiasa Y, Nishiguchi S, Koike A, Sakaida I, Imamura M, Ito K, Yano K, Masaki N, Sugauchi F, Izumi N, Tokunaga K, Mizokami M.** 2009. Genome-wide association of IL28B with response to pegylated interferon-alpha and ribavirin therapy for chronic hepatitis C. Nat. Genet. **41**:1105–1109. http://dx.doi.org/10.1038/ng.449.
82. **Zhou D, Mei Q, Li J, He H.** 2012. Cyclophilin A and viral infections. Biochem. Biophys. Res. Commun. **424**:647–650. http://dx.doi.org/10.1016/j.bbrc.2012.07.024.
83. **Braaten D, Luban J.** 2001. Cyclophilin A regulates HIV-1 infectivity, as demonstrated by gene targeting in human T cells. EMBO J. **20**:1300–1309. http://dx.doi.org/10.1093/emboj/20.6.1300.
84. **Luban J, Bossolt KL, Franke EK, Kalpana GV, Goff Stephen P.** 1993. Human immunodeficiency virus type 1 Gag protein binds to cyclophilins A and B. Cell **73**:1067–1078. http://dx.doi.org/10.1016/0092-8674(93)90637-6.
85. **Tian X, Zhao C, Zhu H, She W, Zhang J, Liu J, Li L, Zheng S, Wen YM, Xie Y.** 2010. Hepatitis B virus (HBV) surface antigen interacts with and promotes cyclophilin a secretion: possible link to pathogenesis of HBV infection. J. Virol. **84**:3373–3381. http://dx.doi.org/10.1128/JVI.02555-09.
86. **Zhao C, Fang CY, Tian XC, Wang L, Yang PY, Wen YM.** 2007. Proteomic analysis of hepatitis B surface antigen positive transgenic mouse liver and decrease of cyclophilin A. J. Med. Virol. **79**:1478–1484. http://dx.doi.org/10.1002/jmv.20945.
87. **Liu X, Sun L, Yu M, Wang Z, Xu C, Xue Q, Zhang K, Ye X, Kitamura Y, Liu W.** 2009. Cyclophilin A interacts with influenza A virus M1 protein and impairs the early stage of the viral replication. Cell Microbiol. **11**:730–741. http://dx.doi.org/10.1111/j.1462-5822.2009.01286.x.
88. **Inoue K, Sekiyama K, Yamada M, Watanabe T, Yasuda H, Yoshiba M.** 2003. Combined interferon α2b and cyclosporin A in the treatment of chronic hepatitis C: controlled trial. J. Gastroenterol. **38**:567–572.
89. **Dorner M, Horwitz JA, Donovan BM, Labitt RN, Budell WC, Friling T, Vogt A, Catanese MT, Satoh T, Kawai T, Akira S, Law M, Rice CM, Ploss A.** 2013. Completion of the entire hepatitis C virus life cycle in genetically humanized mice. Nature **501**:237–241. http://dx.doi.org/10.1038/nature12427.
90. **Ross-Thriepland D, Amako Y, Harris M.** 2013. The C terminus of NS5A domain II is a key determinant of hepatitis C virus genome replication, but is not required for virion assembly and release. J. Gen. Virol. **94**:1009–1018. http://dx.doi.org/10.1099/vir.0.050633-0.
91. **Yang F, Robotham JM, Nelson HB, Irsigler A, Kenworthy R, Tang H.** 2008. Cyclophilin A is an essential cofactor for hepatitis C virus infection and the principal mediator of cyclosporine resistance in vitro. J. Virol. **82**:5269–5278. http://dx.doi.org/10.1128/JVI.02614-07.

Toxicology and Applied Pharmacology 282 (2015) 237–243

Contents lists available at ScienceDirect

Toxicology and Applied Pharmacology

journal homepage: www.elsevier.com/locate/ytaap

Mitochondrial iron accumulation exacerbates hepatic toxicity caused by hepatitis C virus core protein

Shuichi Sekine [a], Konomi Ito [a], Haruna Watanabe [a], Takafumi Nakano [a], Kyoji Moriya [b], Yoshizumi Shintani [b], Hajime Fujie [b], Takeya Tsutsumi [b], Hideyuki Miyoshi [b], Hidetake Fujinaga [b], Seiko Shinzawa [b], Kazuhiko Koike [b], Toshiharu Horie [a,*]

[a] Laboratory of Biopharmaceutics, Graduate School of Pharmaceutical Sciences, Chiba University, 1-8-1 Inohana, Chuo-ku, Chiba 260-8675, Japan
[b] Department of Internal Medicine, Graduate School of Medicine, The University of Tokyo, 7-3-1 Hongo, Bunkyo-ku, Tokyo 113-8655, Japan

ARTICLE INFO

Article history:
Received 8 September 2014
Revised 9 December 2014
Accepted 16 December 2014
Available online 27 December 2014

Keywords:
Ca^{2+} uniporter
Fenton reaction
Reactive oxygen species
Ru360
Hepatitis C virus

ABSTRACT

Patients with long-lasting hepatitis C virus (HCV) infection are at major risk of hepatocellular carcinoma (HCC). Iron accumulation in the livers of these patients is thought to exacerbate conditions of oxidative stress. Transgenic mice that express the HCV core protein develop HCC after the steatosis stage and produce an excess of hepatic reactive oxygen species (ROS). The overproduction of ROS in the liver is the net result of HCV core protein-induced dysfunction of the mitochondrial respiratory chain. This study examined the impact of ferric nitrilacetic acid (Fe-NTA)-mediated iron overload on mitochondrial damage and ROS production in HCV core protein-expressing HepG2 (human HCC) cells (Hep39b cells). A decrease in mitochondrial membrane potential and ROS production were observed following Fe-NTA treatment. After continuous exposure to Fe-NTA for six days, cell toxicity was observed in Hep39b cells, but not in mock (vector-transfected) HepG2 cells. Moreover, mitochondrial iron (^{59}Fe) uptake was increased in the livers of HCV core protein-expressing transgenic mice. This increase in mitochondrial iron uptake was inhibited by Ru360, a mitochondrial Ca^{2+} uniporter inhibitor. Furthermore, the Fe-NTA-induced augmentation of mitochondrial dysfunction, ROS production, and cell toxicity were also inhibited by Ru360 in Hep39b cells. Taken together, these results indicate that Ca^{2+} uniporter-mediated mitochondrial accumulation of iron exacerbates hepatocyte toxicity caused by the HCV core protein.

Introduction

Hepatitis C virus (HCV) infection is a major cause of chronic liver disease. About 120–200 million people are infected with HCV, increasing their risk of developing chronic hepatitis, cirrhosis, and eventually hepatocellular carcinoma (HCC) (Ikeda et al., 1998; Nishioka et al., 1991). The HCV genome is approximately 9.6 kb in size and encodes a polyprotein of ~3000 amino acids. The large HCV polyprotein is cleaved by host and viral proteases to generate at least ten smaller proteins, including four structural proteins (one core protein, two envelope proteins, and the E1, E2, and p7 ion channels) (Bukh et al., 1995) and six non-structural proteins (NH2-NS2, NS3, NS4A, NS4B, NS5A, and NS5B-COOH) (Bartenschlager and Lohmann, 2000). These proteins participate in viral replication and also influence cellular functions of the host.

Oxidative stress is commonly observed following HCV infection and is caused by increased levels of cellular reactive oxygen species (ROS) or by changes in cellular antioxidant capacities (Choi and Ou, 2006; Oberley, 2002; Otani et al., 2005). In particular, HCV core protein is known to be closely associated with the mitochondria and causes the increase in host ROS production, lipid peroxidation (Lau et al., 1998; Moriya et al., 2001; Okuda et al., 2002) and mitochondrial Ca^{2+} uptake. HCV core protein also reduces GSH and NADPH concentrations and mitochondrial complex I activities. These undertakings ultimately disrupt mitochondrial membrane permeability and trigger mitochondrial dysfunction (Wang et al., 2010; Wang and Weinman, 2006). As mitochondrial function is the master regulator of cellular energy and apoptotic cell death, mitochondrial injury can culminate in metabolic deficits and steatohepatitis, further exacerbating cell injury and dysfunction.

Due to the relationship between chronic HCV infection and the development of HCC, numerous studies have attempted to identify the HCV proteins that are responsible for hepatocarcinogenesis. These studies indicate that the HCV core protein can promote the immortalization of primary human hepatocytes (Ray et al., 2000), whereas the non-

Abbreviations: HCV, hepatitis C virus; HCC, hepatocellular carcinoma; ROS, reactive oxygen species; Fe-NTA, ferric nitrilacetic acid; JC-1, 5,5′,6,6′-tetrachrolo-1,1′,3,3′-tetraethylbenzimidazoly-carbocyanine iodide; CCCP, carbonyl cyanide-m-chlorophenyl hydrazine; MTT, 3-(4,5-dimethylthiazol-2-yl)-2,5-diphenyltetrazolium bromide; HPF, hydroxyphenyl fluorescein; ANT, adenine nucleotide translocator; HRP, horseradish peroxidase; DMEM, Dulbecco's Modified Eagle's Medium; CL, chemiluminescence; TTBS, Tris-buffered saline/0.05% Tween 20; BSA, bovine serum albumin; Hep39b, HCV core protein-expressing HepG2; Hepswx, vector-transfected HepG2.

* Corresponding author at: Faculty of Pharmaceutical Sciences, Teikyo Heisei University, 4-21-2 Nakano, Nakano-ku, Tokyo 164-8530, Japan. Fax: +81 3 5860 4237.
E-mail address: t.horie@thu.ac.jp (T. Horie).

http://dx.doi.org/10.1016/j.taap.2014.12.004
0041-008X/

structural proteins NS3 and NS4B can transform NIH 3T3 cells, either individually or in combination with Ha-ras (Park et al., 2000). Iron overload in the liver, which is associated with the genetic disorder hereditary hemochromatosis, has been thought to increase the risk of HCC by about 200-fold (Bonkovsky et al., 1997; Kowdley, 2004). For example, the livers of patients afflicted with HCV are characterized by the elevated expression of transferrin receptor 1 and hepcidin, both of which stimulate iron uptake into hepatocytes (Bonkovsky et al., 1997; Hayashi et al., 1994). In contrast, iron depletion (in the form of dietary iron restriction and/or phlebotomy) can improve hepatic inflammation and lower serum aminotransferase activity in HCV patients (Hayashi et al., 1994). Thus, a major precipitating factor for the pathogenesis of HCV-related liver disease has been attributed to the augmentation of oxidative stress following iron accumulation. However, no underlying cellular mechanism has yet been elucidated.

This study investigated the effect of iron exposure on mitochondrial dysfunction, ROS production and cell toxicity in human hepatoma cells stably expressing the HCV core protein (Hep39b cells). The underlying mechanism responsible for mitochondrial iron accumulation in Hep39b cells and in the livers of HCV core protein-expressing transgenic mice was also examined.

Materials and methods

Chemicals and reagents. Ferric nitrate nonahydrate, nitrilotriacetic acid (NTA), 5,5′,6,6′-tetrachrolo-1,1′,3,3′-tetraethylbenzimidazolycarbocyanine iodide (JC-1), carbonyl cyanide-m-chlorophenyl hydrazine (CCCP) and G418 disulfate were from Sigma Aldrich (St. Louis, MO). MitoTracker® Red was from Invitrogen (Carlsbad, CA). $^{59}FeSO_4$ was from Perkin-Elmer (Waltham, MA). Ru360 was from Merck Millipore Japan (Tokyo, Japan). MTT [3-(4,5-dimethylthiazol-2-yl)-2,5-diphenyltetrazolium bromide] was from Wako Pure Chemical Industries, Ltd. (Osaka, Japan). Hydroxyphenyl fluorescein (HPF) was from Sekisui Medical Co., Ltd. (Tokyo, Japan). Adenine nucleotide translocator (ANT) goat polyclonal IgG, CCDC109A goat polyclonal IgG and horseradish peroxidase (HRP)-conjugated anti-goat IgG were from Santa Cruz Biotechnology, Inc. (Santa Cruz, CA). All chemicals and solvents were of analytical grade.

Preparation of Fe-NTA. The Fe-NTA complex was prepared as described by Awai et al. (1979). Briefly, ferric nitrate was dissolved in 1 N HCl to form a 50 mM solution, and NTA was dissolved in 1 N NaOH to form a 150 mM solution. Equal volumes of the two solutions were mixed just before the experiment, and the pH was adjusted to 7.4 with $NaHCO_3$.

Assessment of cytotoxicity. Cytotoxicity was assessed by the MTT assay. Briefly, Hep39b and Hepswx cells were seeded into 96 well culture plates at a density of 8.4×10^3 cells/well and were exposed to various concentrations of Fe-NTA the following day, the medium was replaced with fresh medium containing the same component every 24 h. In some conditions, cells were treated with 20 μM Ru360, a mitochondrial Ca^{2+} uniporter inhibitor, for 1 h prior to Fe-NTA exposure. After six days, the cell culture medium was replaced by 50 μl MTT solution (5 mg/ml MTT in phenol red-free Dulbecco's Modified Eagle's Medium (DMEM)), and the cells were incubated for 2 h at 37 °C. To dissolve the reduced MTT crystals, 200 μl isopropanol was added. The absorbance of the dye was measured at a wavelength of 570 nm, and the turbidity of the cells (background absorbance) was measured at a reference wavelength of 630 nm. The absorbance of the controls (Hepswx and Hep39b) was set at 100%, and cytotoxicity was calculated as the absorbance of the experimental sample relative to that of the control.

Assessment of ROS production. ROS production was first assessed by chemiluminescence (CL) analysis. Briefly, cells were seeded into 35 mm glass-bottomed dishes at a density of 2.5×10^5 cells/dish and exposed to 300 μM Fe-NTA the following day, the medium was replaced with fresh medium containing the same component every 24 h. In some cases, cells were treated with Ru360 for 1 h prior to Fe-NTA treatment. After five days, the cell culture medium was replaced with phenol red-free DMEM containing Fe-NTA and Ru360, and the dish was protected from light. The following day, spontaneous CL was measured using a single photoelectron counting system (CLD-10; Tohoku Electronic Industrial Co., Ltd., Sendai, Japan), as described previously (Maeda et al., 2010). Emission was expressed in counts/10 min/mg protein.

ROS production was also assessed using HPF as a fluorescent probe for the selective detection of hydroxyl radicals. Briefly, cells were seeded into 35 mm glass-bottomed dishes, as described for CL analysis. After 7 days, the cell culture medium was replaced with modified Hanks' balanced salt solution (HBSS) containing 10 mM HEPES, 1 mM $MgCl_2$, 2 mM $CaCl_2$ and 2.7 mM glucose (pH 7.4). Next, 10 μM HPF and 20 nM MitoTracker® Red (a fluorescent probe for the mitochondria) were added, and cells were incubated for 15 min at 37 °C. Images of HPF and MitoTracker® Red staining were obtained using a laser scanning confocal microscope (FV300; Olympus Optical Co., Ltd., Tokyo, Japan). The wavelengths (excitation/emission) for the detection of HPF (green) and MitoTracker® Red (red) were 488 nm/515 nm and 579 nm/599 nm, respectively.

Assessment of mitochondrial membrane potential. Measurement of mitochondrial membrane potential was performed using the JC-1 stain, a lipophilic cation fluorescent dye that accumulates in the mitochondria. At a low mitochondrial membrane potential, the JC-1 dye exists as a monomeric molecule and fluoresces green, whereas at a higher membrane potential the JC-1 dye forms polymeric aggregates and fluoresces red. A fall in the mitochondrial membrane potential is therefore indicated by a decrease in the ratio of red signal to green signal.

Cells were cultured in 96 well black culture plates at a density of 8.4×10^3 cells/well and exposed to various concentrations of Fe-NTA the following day, the medium was replaced with fresh medium containing the same component every 24 h. After six days, the culture medium was replaced with 200 μl JC-1 solution (10 μg/ml JC-1 in HBSS), and cells were incubated in the dark for 30 min at 37 °C. After washing twice with HBSS, the absorbance of the cells in each well was immediately measured using a fluorescence plate reader with the excitation and emission wavelengths set at 490 nm and 530 nm (green)/590 nm (red), respectively.

Animals. The production of transgenic mice expressing the HCV core protein has been described previously (Moriya et al., 2001). Briefly, the HCV core protein gene was placed downstream of a transcriptional regulatory region from the hepatitis B virus and introduced into C57BL/6 mouse embryos (Clea Japan, Tokyo, Japan). All of the animals were treated humanely in accordance with the guidelines issued by the National Institute of Health and all procedures described below were approved by the animal care committee of Chiba University.

Isolation of mouse liver mitochondria. The mouse liver mitochondrial fraction was prepared according to a previously described method (Masubuchi et al., 2002). Livers were isolated from two mice and placed in ice-cold buffer containing 250 mM sucrose, 10 mM HEPES–KOH, and 0.5 mM EGTA (pH 7.4). Livers were cut into small cubes with scissors in the same buffer and homogenized five times with a Potter homogenizer. The homogenates were diluted to 0.25 g liver/ml and were centrifuged at 770 ×*g* for 5 min at 4 °C. The resulting supernatant was decanted and further centrifuged at 9800 ×*g* for 10 min. The pellet was resuspended to yield a concentration of 0.5 g liver/ml in buffer containing 250 mM sucrose, 10 mM HEPES–KOH and 0.3 mM EGTA (pH 7.4), and centrifuged at 4500 ×*g* for 10 min. The pellet was resuspended to yield a concentration of 1 g liver/ml in the same buffer and centrifuged at 2000 ×*g* for 2 min, followed by further centrifugation at 4500 ×*g* for 8 min. The

final pellet was then resuspended in buffer containing 250 mM sucrose and 10 mM HEPES–KOH (pH 7.4) and used for further experiments.

Mitochondrial iron uptake. All experiments were conducted in a 30 °C water bath. After pre-incubation of the mitochondria in buffer containing 225 mM sucrose, 10 mM KCl, 5 mM $MgCl_2$, 5 mM KH_2PO_4, and 20 mM Tris–HCl (pH 7.4) for 1 min, Ru360 was added at a final concentration of 10 μM, $^{59}FeSO_4$ was added after 1 min, and the ^{59}Fe remaining in the mitochondria after 10 min was measured using a gamma counter.

Western blotting analysis. The mouse liver mitochondrial fraction (10 μg protein) was subjected to electrophoresis on a 12.5% polyacrylamide slab gel containing 0.1% sodium dodecyl sulfate and transferred onto an Immobilon-P Transfer Membrane filter (Millipore Corporation, Billerica, MA). The membrane was blocked for 1 h at room temperature with Tris-buffered saline/0.05% Tween 20 (TTBS) containing 3% bovine serum albumin (BSA) and probed overnight at 4 °C with the CCDC109A goat polyclonal IgG (1:200) against the Ca^{2+} uniporter and the ANT goat polyclonal IgG (1:1000). The membrane was then incubated for 1 h at room temperature with donkey anti-goat IgG-HRP (1:3333). All antibodies were diluted in TTBS containing 0.1% BSA. Immunoreactive bands were detected using a LAS-1000 imaging system (Fuji Film, Tokyo, Japan) and an enhanced CL system (GE Healthcare, Little Chalfont, Buckinghamshire, UK).

Statistical analysis. All data are represented as the mean ± the standard error (S.E.). Data were statistically analyzed by using one-way ANOVA followed by the Bonferroni test for multiple comparison. For comparison among two groups, two-tailed Student's t-test was adopted. Differences between means at the level of $P < 0.05$ were considered significant.

Results

Iron-induced cytotoxicity in HCV core protein-expressing HepG2 cells

The iron uptake system is perturbed in HCV-infected hepatocytes due to elevated expression of transferrin receptor 1. However, because of its hydrophobicity, Fe-NTA is taken up into the cell in a transferrin receptor 1-independent manner by passive diffusion. Fe-NTA is then converted into free Fe^{2+} by several types of esterases. Therefore, Fe-NTA was used in the current study to control for intrinsic differences in active iron uptake between HCV core protein-expressing HepG2 cells (Hep39b cells) and vector-transfected HepG2 cells (Hepswx cells). After treatment with Fe-NTA for six days, cytotoxicity was assessed using the MTT assay. Concentration-dependent cytotoxicity of Fe-NTA against Hep39b cells was observed. By contrast, no cytotoxicity was observed against control Hepswx cells at Fe-NTA concentrations of less than 1000 μM (Fig. 1). These data indicate that HCV core protein expression affects the susceptibility of hepatocytes to Fe-NTA-induced iron cytotoxicity.

Effect of iron accumulation on ROS production in HCV core protein-expressing versus control hepatocytes

To directly measure free radical formation, we took advantage of methodology for measuring spontaneous CL and compared the levels of CL in HCV core protein-expressing Hep39b and control Hepswx cells (Fig. 2a). As shown in Fig. 2a, spontaneous CL was significantly higher in Hep39b cells by approximately 156% compared with that in Hepswx cells (6015 versus 3856 arbitrary units; $P < 0.01$). In the presence of 300 μM Fe-NTA, iron-induced CL was also significantly higher in Hep39b cells relative to Hepswx cells (2.61-fold versus 1.54-fold increase; $P < 0.01$ and $P < 0.001$, respectively) (Fig. 2a).

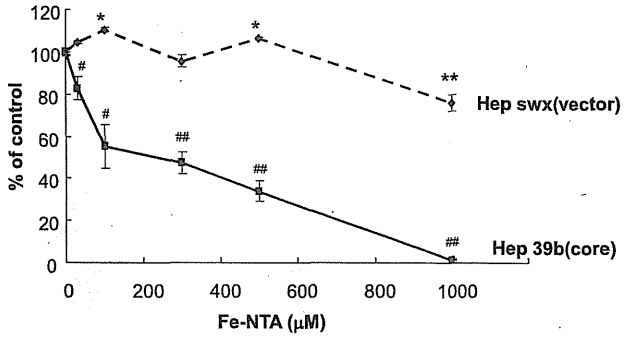

Fig. 1. Iron-induced cytotoxicity in control versus HCV core protein-expressing hepatocytes. Hepswx (dashed line) and Hep39b (solid line) cells were exposed with Fe-NTA (30, 100, 300, 500 and 1000 μM) for six days. Hepatotoxicity was determined using the MTT assay. Viability was calculated as the absorbance of the experimental sample relative to that of the controls (without Fe-NTA treatments). Values are the mean ± the S.E. $^{*}P < 0.05$ and $^{**}P < 0.01$, significantly different from the control (without Fe-NTA). $^{\#}P < 0.05$ and $^{\#\#}P < 0.01$, significantly different from respective control cells (Hepswx) ($n = 6$).

Effect of iron accumulation on mitochondrial ROS production

Mitochondria are a major source of ROS production. Therefore, we next examined the production of mitochondrial hydroxyl radicals by free iron catalyzation (i.e., the Fenton reaction). Since increased production of ROS was observed in Hep39b cells in the presence of Fe-NTA, we next examined mitochondrial ROS production by double staining with MitoTracker® Red (red), a fluorescent probe for the mitochondria, and HPF (green), a fluorescent probe for the selective detection of hydroxyl radicals. As shown in Fig. 2b, a strong fluorescent signal derived from HPF was observed in Hep39b cells in the presence of Fe-NTA. This fluorescence overlapped with that generated by MitoTracker® Red (Fig. 2b). The fluorescent signal derived from HPF in overlapped area was significantly higher in Hep39b cells by approximately 200% compared with that in Hepswx cells (Fig. 2c). These data indicate that mitochondrial hydroxyl radical production was increased in the presence of the HCV core protein and Fe-NTA.

Effect of HCV core protein on mitochondrial membrane potential

The HCV core protein is known to inhibit mitochondrial respiratory complex I activity (Korenaga et al., 2005). Inhibition of complex I leads to ROS formation due to premature electron leakage from the complex. Therefore, we next examined the effect of Fe-NTA on mitochondrial membrane potential in Hep39b cells by using JC-1, a lipophilic cationic dye that selectively enters the mitochondria and reversibly changes color from green to red as the membrane potential increases. Fig. 3 demonstrates that the mitochondrial membrane potential was decreased in HCV core protein-expressing Hep39b cells compared with control Hepswx cells. The decrease in membrane potential was significantly increased following exposure to Fe-NTA (300 and 1000 μM) for six days (Fig. 3).

Mitochondrial free iron uptake in HCV core protein-expressing versus control hepatocytes

Because mitochondrial hydroxyl radical production was increased in the presence of Fe-NTA (Fig. 2), the uptake of free iron into isolated mitochondria was next examined. To ensure a sufficient quantity and quality of the mitochondria for this experiment, mitochondria were isolated from the liver of HCV core protein-expressing transgenic and wild-type (control) mice. Fig. 4 shows that the concentration of mitochondrial free

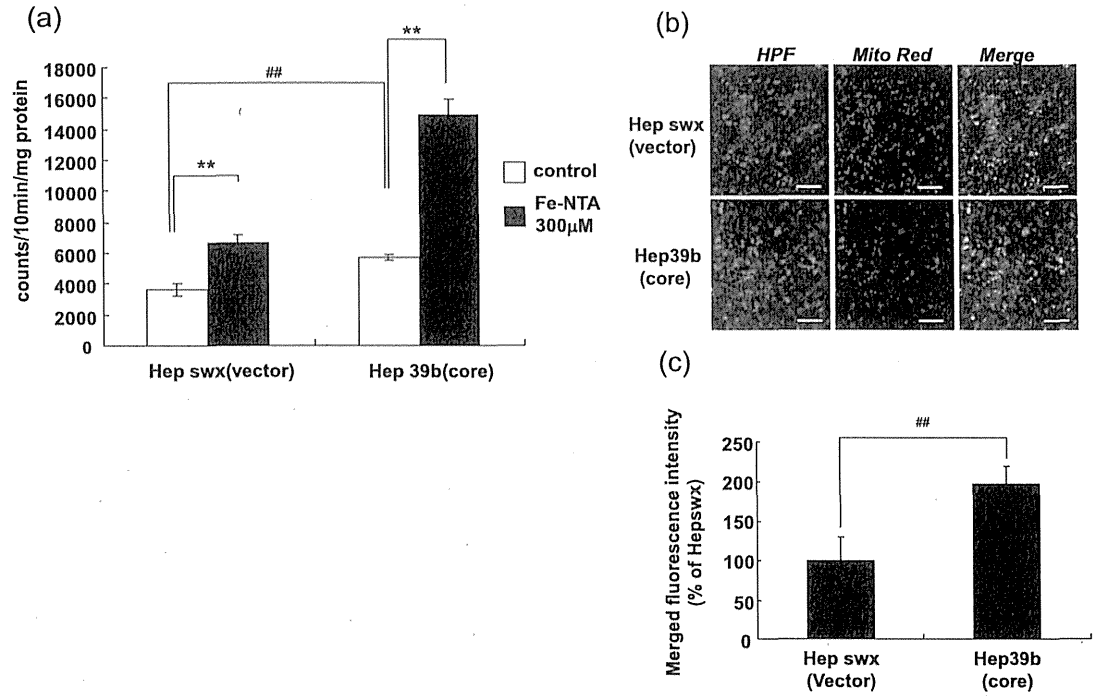

Fig. 2. Iron-induced mitochondrial ROS production is enhanced in HCV core protein-expressing hepatocytes. (a) Hepswx and Hep39b cells were exposed to Fe-NTA (300 μM) for six days. ROS production was determined using a CL analyzer. Detected counts were normalized by protein content of cell lysate. Values are given as the mean ± the S.E. $^{**}P < 0.01$ and $^{\#\#}P < 0.01$, significantly different from respective control (n = 3–4). (b) Hepswx and Hep39b cells were pretreated with HPF (green) and MitoTracker® Red (red). Mitochondrial ROS production was determined by the strength of yellow fluorescence in the merged pictures. The scale bar represents 100 μm. (c) Analysis of merged fluorescence microscopy images was done by ImageJ. Integrated density of merged area was automatically selected and fluorescence intensity of HPF was calculated within the merged area of 200–300 cells.

iron ($^{59}Fe^{2+}$) was significantly increased in the mitochondria derived from the transgenic versus the control mouse liver (62.2 ± 4.2 versus 79.5 ± 2.1 pmol/mg protein, respectively; $P < 0.05$), whereas the passive diffusion of $^{59}Fe^{2+}$ into the mitochondria (estimated by $^{59}Fe^{2+}$ uptake at 4 °C) was 31.1 ± 3.2 pmol/10 min/mg protein in Hepswx cells, and 29.2 ± 1.8 pmol/10 min/mg protein in Hep39b cells (not significantly different). Moreover, $^{59}Fe^{2+}$ uptake into the transgenic and control mitochondria was attenuated to the same level by Ru360 (48.2 ± 4.1 versus 47.5 ± 1.2 pmol/mg protein, respectively) (Fig. 4). These data indicate that calcium uniporter plays a role in free iron uptake into the mitochondria and that the activity of the Ca^{2+} uniporter is increased by the HCV core protein.

Effect of Ru360 on Fe-NTA-induced ROS production and cytotoxicity

We next examined the effect of Ru360 on Fe-NTA-induced ROS production and cytotoxicity in Hep39b versus Hepswx cells. As shown in Fig. 5a, in the absence of Fe-NTA, Ru360 had no effect on ROS production

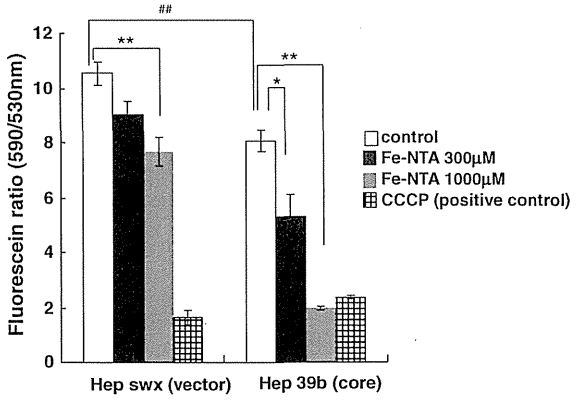

Fig. 3. The iron-induced reduction in mitochondrial membrane potential is increased by the expression of HCV core protein. Hepswx and Hep39b cells were exposed to Fe-NTA for six days. Mitochondrial membrane potential was estimated fluorometrically. Values are given as the mean ± the S.E. $^{*}P < 0.05$, $^{**}P < 0.01$ and $^{\#\#}P < 0.01$, significantly different from respective control (n = 6).

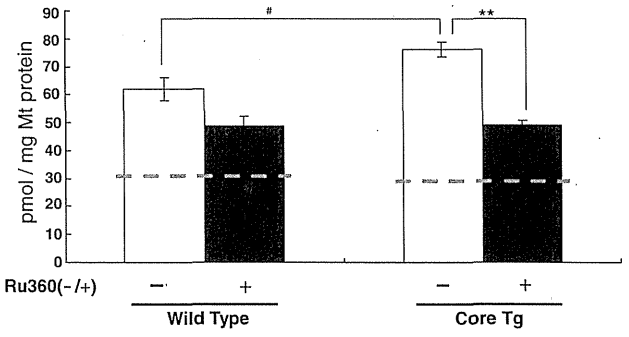

Fig. 4. Mitochondrial iron uptake is augmented by the expression of HCV core protein and inhibited by Ru360. Mitochondria were isolated from wild-type and HCV core protein transgenic (Tg) mice and exposed to $^{59}FeSO_4$ with/without Ru360. Free iron uptake was measured in the isolated mitochondria and the free iron uptake amount was normalized by mitochondrial protein content. The dashed line represents the passive diffusion into the mitochondria. Values are given as the mean ± the S.E. $^{**}P < 0.01$ and $^{\#}P < 0.05$, significantly different from respective control (n = 3–8).

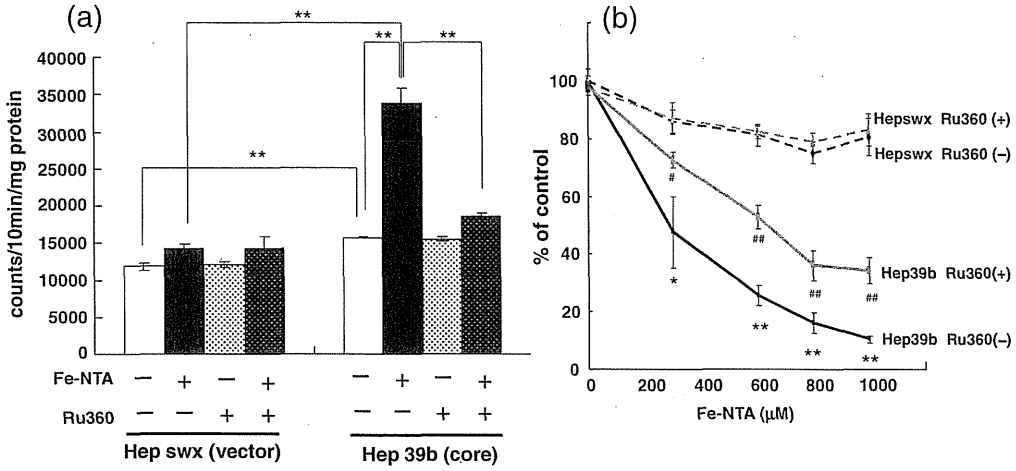

Fig. 5. Iron-induced ROS production and cytotoxicity are inhibited by Ru360 in HCV core protein-expressing hepatocytes. (a) Hepswx and Hep39b cells were exposed to Fe-NTA (300 μM) and Ru360 (20 μM) for six days. ROS production was determined using a CL analyzer. Values are given as the mean ± the S.E. **P < 0.01, significantly different from respective control (n = 8). (b) Hepswx and Hep39b cells were exposed to Fe-NTA (300, 600, 800, and 1000 μM) and Ru360 (20 μM) for six days. Cytotoxicity was determined using the MTT assay. Values are given as the mean ± the S.E. *P < 0.05 and **P < 0.01, significantly different from Hepswx Ru360(−). #P < 0.05 and ##P < 0.01, significantly different from Hep39b Ru360(−) (n = 6).

in Hepswx cells and Hep39b cells. On the other hand, Ru360 significantly suppressed Fe-NTA (300 μM)-induced ROS production in Hep39b but not Hepswx cells (Fig. 5a). Moreover, cytotoxicity following exposure to (300, 600, 800 and 1000 μM) Fe-NTA for six days was also specifically inhibited by Ru360 treatment in Hep39b cells (Fig. 5b).

Expression of the Ca^{2+} uniporter in isolated mitochondria

Given that mitochondrial free iron uptake is enhanced in HCV core protein-expressing Hep39b cells (Fig. 4), we next examined the expression of the Ca^{2+} uniporter in the mitochondria isolated from the liver of HCV core protein-expressing transgenic mice relative to control mice. As shown in Fig. 6, mitochondrial expression of the uniporter was similar in transgenic versus control mice, as assessed by Western blot analysis.

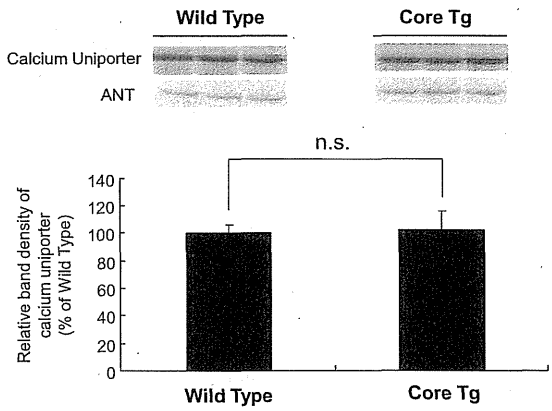

Fig. 6. Expression of mitochondrial Ca^{2+} uniporter in the livers of HCV core protein-expressing transgenic versus wild-type mice. Mitochondria were isolated from the livers of wild-type (control) and HCV core protein-expressing transgenic (Tg) mice. The expression levels of the Ca^{2+} uniporter and ANT (loading control) were determined by Western blot analysis. Mitochondrial proteins (10 μg) were loaded into each lane of the gel. The band density of the uniporter was normalized to the band density of ANT. Values are given as the mean ± the S.E. n.s.: not significantly different (n = 3).

Discussion

The accumulation of iron into the liver of HCV core protein-expressing transgenic mice fed a normal diet is similar to that observed in chronic HCV patients (Farinati et al., 1995; Kato et al., 2001). On the other hand, the expression level of hepcidin, which regulates iron metabolism by inhibiting iron absorption from the intestine and the hepatic portal system, is reportedly decreased in the liver of HCV patients and full-length HCV genome-expressing transgenic mice, but not in the liver of HCV core protein-expressing transgenic mice (Moriya et al., 2010; Muckenthaler, 2008). Therefore, although the precise regulation of iron transport into the mitochondria is essential for heme biosynthesis, hemoglobin production, and Fe–S clustering, the mechanism(s) behind mitochondrial iron homeostasis is not yet fully understood.

Previous work from our group revealed elevated ROS generation in HCV core protein-expressing transgenic mice (Moriya et al., 2001). Moreover, our previous work, along with that of others (Korenaga et al., 2005), showed that the core protein interacts with the outer mitochondrial membrane and impairs the mitochondrial respiratory chain in the normal mouse liver via inhibition of complex I activity (unpublished data). Inhibition of respiratory chain complexes ultimately leads to the overproduction of ROS via electron leakage from the mitochondria. Therefore, we hypothesized that the inducible mitochondrial iron transport system exacerbates hepatic toxicity caused by the HCV core protein.

This study employed Fe-NTA to exclude intrinsic differences in iron uptake into HCV core protein-expressing Hep39b cells and vector-transfected Hepswx cells. In addition, we demonstrated that HCV core protein-induced alterations in mitochondrial ROS production and membrane potential were augmented in the presence of iron (Figs. 2 and 3). These data may indicate that iron-dependent mitochondrial dysfunction was amplified via the Fenton reaction, which produces potent reactive free radicals (i.e., hydroxyl radicals) (Fig. 7).

Iron is absolutely essential for the sustenance of all forms of life due to its unusual ability to serve as both an electron donor and acceptor. On the other hand, free iron is also potentially toxic, which is related to its ability to donate and accept electrons within the cell. Free iron catalyzes the conversion of hydrogen peroxide into free radicals, which can cause damage to the mitochondria and cellular structures. For this reason, the iron homeostasis is strictly regulated, and the impairment of iron homeostasis is related to several diseases. In patients with HCV, hepatic

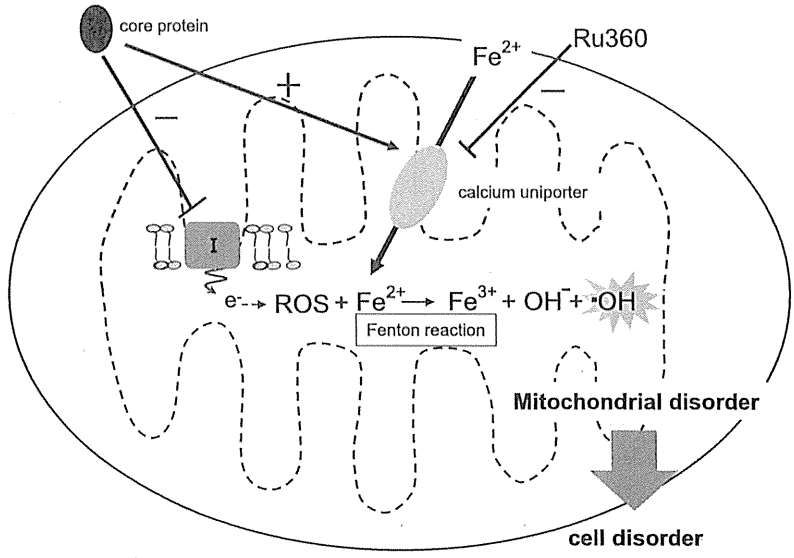

Fig. 7. Proposed mechanism of mitochondrial iron accumulation and hepatic cytotoxicity caused by the HCV core protein. The HCV core protein induces mitochondrial ROS production by inhibiting mitochondrial complex I. In addition, it is suggested that the HCV core protein stimulates mitochondrial iron uptake through the mitochondrial Ca^{2+} uniporter. The excess iron then leads to mitochondrial ROS production and mitochondrial/cellular malfunction/disorder when the HCV core protein is expressed.

and serum free iron concentrations are ~7-fold higher (12.5 mmol/g liver and 134 mg/dl, respectively) than those of a normal individual (Farinati et al., 1995; Kageyama et al., 1998; Olynyk et al., 1995; Silva et al., 2005). In this study, significant hepatotoxicity was observed at 30 μM Fe-NTA in HCV core protein-expressing Hep39b cells (Fig. 1). Therefore, a physiologically relevant concentration of iron (30 μM), which is not sufficient to induce cell toxicity by itself, was synergistic with the toxic actions of the core protein (Fig. 1). This interplay was similarly revealed by the synergy between iron and the core protein in inducing mitochondrial dysfunction and ROS production (Figs. 2 and 3).

This study further demonstrated that mitochondrial free iron uptake was partially mediated by the Ca^{2+} uniporter. The Ca^{2+} uniporter was selectively inhibited by Ru360 and exhibited an increased capacity to uptake iron into HCV core protein-expressing liver mitochondria versus normal liver mitochondria (Fig. 4). However, the expression of the uniporter was unaltered in core protein-expressing transgenic mice relative to normal mice (Fig. 6). Li et al. (2007) reported that the activity of the Ca^{2+} uniporter was up-regulated in the presence of the core protein: The in vitro incubation of mouse liver mitochondria with HCV core protein (100 ng/mg) increased the Ca^{2+} entry rate by ~2-fold. The Ca^{2+} uniporter is located in the inner mitochondrial membrane and transports not only Ca^{2+} but also other metal cationic ions (e.g., Fe^{2+}) into the mitochondrial matrix space in a mitochondrial membrane potential-dependent fashion (Bernardi, 1999).

Iron uptake was significantly suppressed to the same level by Ru360 in the mitochondria isolated from both core protein-expressing transgenic and normal mice (Fig. 4). Moreover, as free iron uptake into the mitochondria was still observed at 4 °C for both types of the mitochondria, about half of the iron (Hepswx; 31.1 ± 3.2 pmol/10 min/mg protein, Hep39b; 29.2 ± 1.8 pmol/10 min/mg protein) was estimated to enter into the mitochondria by passive diffusion (Fig. 4, dashed line). These data indicate that the up-regulation of iron uptake in the mitochondria isolated from transgenic mice was mediated by the HCV core protein-induced stimulation of Ru360-sensitive Ca^{2+} uniporter transport activity. However, the mechanism by which the core protein alters the function of the mitochondrial uniporter is still unclear, especially given that the core protein binds to the outer mitochondrial membrane, and the uniporter is located in the inner mitochondrial membrane. It is known that mitochondrial calcium uniporter possibly forms multi-molecular complex (Raffaello et al., 2012). Mitochondrial calcium uniporter function could be altered by the effect on essential regulator and/or protein involved in the assembly of the channel. In this regard, though our current study demonstrated that HCV core protein had no effect on Ca^{2+} uniporter expression (Fig. 6), it is possible that other mechanisms are involved in the HCV core protein-induced stimulation of Ca^{2+} uniporter transport activity. Further study should be addressed in the future.

Interferon-α has been used as monotherapy for chronic hepatitis C, yet only about 40–50% of hepatitis C patients experience an initial biochemical response to the cytokine. Interestingly, high iron accumulation in chronic HCV carriers is related to a poor response to interferon therapy (Walters et al., 1973). In addition, some investigators have suggested that iron removal therapy (via phlebotomy or food therapy (i.e., restriction of an iron rich-diet)) can attenuate liver damage in hepatitis C patients by still unknown mechanisms (Hayashi et al., 1994; Kato et al., 2007). The current study showed that the HCV core protein-induced mitochondrial iron uptake is responsible for exacerbating mitochondrial dysfunction and ROS production, which finally seems to lead to hepatocyte toxicity (Fig. 7). Based on these results, we suggest that inhibition of the mitochondrial Ca^{2+} uniporter may provide a new therapeutic approach to treat liver disease in HCV patients.

Conflict of interest statement

The authors declare no conflict of interest.

Acknowledgments

This work was supported by a grant-in-aid for scientific research (A) 548 (21249003) and a grant-in-aid for young scientists (B) (21790141) from the Ministry of Education, Culture, Sports, Science and Technology of Japan.

References

Awai, M., Narasaki, M., Yamanoi, Y., Seno, S., 1979. Induction of diabetes in animals by parenteral administration of ferric nitrilotriacetate. A model of experimental hemochromatosis. Am. J. Pathol. 95, 663–673.